Supplementary information

Efficient recovery of rare earth elements (Pr(III) and Tm(III)) from mining residues using a new phosphorylated hydrogel (Algal biomass/PEI)

Chunlin HE,[1] Khalid A.M. SALIH,[1] Yuezhou WEI,[1,2] Hamed MIRA [3], Adel A-H ABDEL-RAHMAN[4], Khalid Z. ELWAKEEL,[5,6] Mohammed F. HAMZA,[1,3*] Eric GUIBAL[7*]

[1] Guangxi Key Laboratory of Processing for Non-ferrous Metals and Featured Materials, School of Resources, Environment and Materials, Guangxi University, Nanning 530004, PR China.
[2] School of Nuclear Science and Technology, Shanghai Jiao Tong University, Shanghai, PR China.
[3] Nuclear Materials Authority, POB 530, El-Maadi, Cairo, Egypt.
[4] Faculty of Science, Menoufia University, Shebine El-Koam, Egypt
[5] Environmental Science Department, Faculty of Science, Port-Said University, Port-Said, Egypt
[6] University of Jeddah, College of Science, Department of Chemistry, Jeddah, Saudi Arabia
[7] IMT – Mines Ales, Polymers Composites and Hybrids (PCH), F-30319 Alès cedex, France

Table S1a. Modeling of uptake kinetics [1-3].

Model	Equation	Parameters	Ref.
PFORE	$q(t) = q_{eq,1}(1 - e^{-k_1 t})$	$q_{eq,2}$ (mmol g^{-1}): sorption capacity at equilibrium k_1 (min^{-1}): apparent rate constant of PFORE	[1]
PSORE	$q(t) = \frac{q_{eq,2}^2 k_2 t}{1 + k_2 q_{eq,2} t}$	$q_{eq,2}$ (mmol g^{-1}): sorption capacity at equilibrium k_2 (g $mmol^{-1}$ min^{-1}): apparent rate constant of PSORE	[1]
Elovich	$q(t) = \frac{1}{\beta} ln(1 + \alpha \times \beta \times t)$	α is the initial rate of sorption (mmol g^{-1} min^{-1}) β is the desorption constant (mmol g^{-1})	[3]
RIDE	$\frac{q(t)}{q_{eq}} = 1 - \sum_{n=1}^{\infty} \frac{6\alpha(\alpha+1)\exp\left(\frac{-D_e q_n^2}{r^2} t\right)}{9 + 9\alpha + q_n^2 \alpha^2}$ With q_n being the non-zero roots of $\tan q_n = \frac{3 q_n}{3 + \alpha q_n^2}$ and $\frac{m q}{V C_0} = \frac{1}{1+\alpha}$	D_e(m^2 min^{-1}) : Effective diffusivity coefficient	[2]

(m (g): mass of sorbent; V (L): volume of solution; C_0 (mmol L^{-1}): initial concentration of the solution).

Table S1b. Modeling of sorption isotherms [1, 2, 4, 5]

Model	Equation	Parameters	Ref.
Langmuir	$q_{eq} = \frac{q_{m,L} C_{eq}}{1 + b_L C_{eq}}$	$q_{m,L}$ (mmol g^{-1}): Sorption capacity at saturation of monolayer b_L (L $mmol^{-1}$): Affinity coefficient	[1]
Freundlich	$q_{eq} = k_F C_{eq}^{1/n_F}$	k_F and n_F: empirical parameters of Freundlich equation	[4]
Sips	$q_{eq} = \frac{q_{m,S} b_S C_{eq}^{1/n_S}}{1 + b_S C_{eq}^{1/n_S}}$	$q_{m,L}$, b_S and n_S: empirical parameters of Sips equation (based on Langmuir and Freundlich equations)	[2]
Temkin	$q_{eq} = \frac{RT}{B_T} \ln(A_T C_{eq})$	T (K); R: gas constant; A_T: Temkin binding constant (L $mmol^{-1}$); B_T: sorption heat (J mol^{-1})	[5]

Akaike Information Criterion, AIC [6]:

$$AIC = N \ln\left(\frac{\sum_{i=0}^{N}\left(y_{i,exp.} - y_{i,model}\right)^2}{N}\right) + 2N_p + \frac{2N_p(N_p+1)}{N - N_p - 1}$$

Where N is the number of experimental points, N_p the number of model parameters, $y_{i,exp.}$ and $y_{i,model}$ the experimental and calculated values of the tested variable.

Table S2a. SEM-EDX of raw beads (APEI)/surface and crosscut section (bar: 200 µm).

SEM	EDX
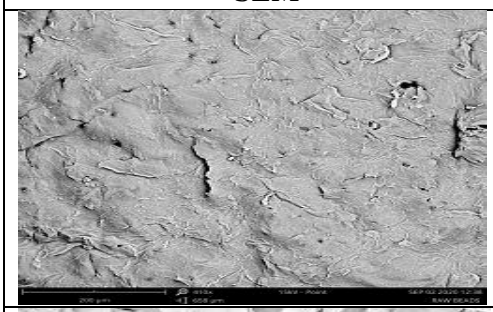	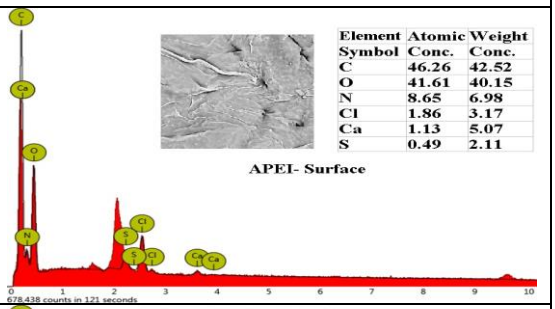
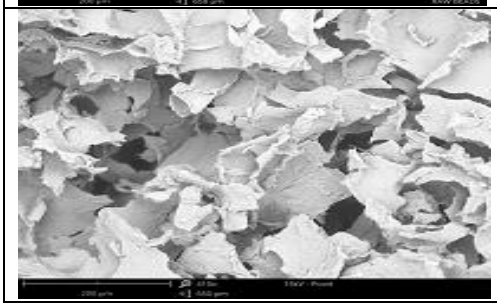	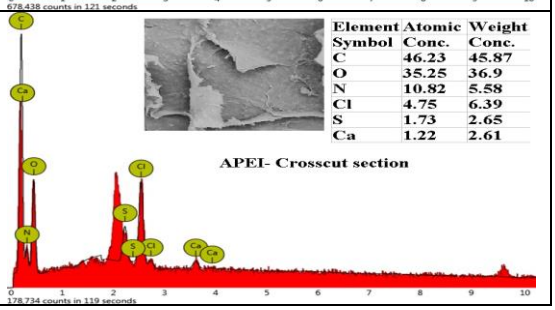

Table S2b. SEM-EDX analysis of activated chloride beads (spacer arm)/surface and crosscut section (bar: 200 µm).

SEM	EDX
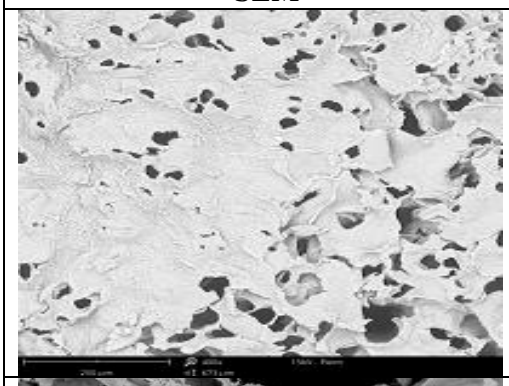	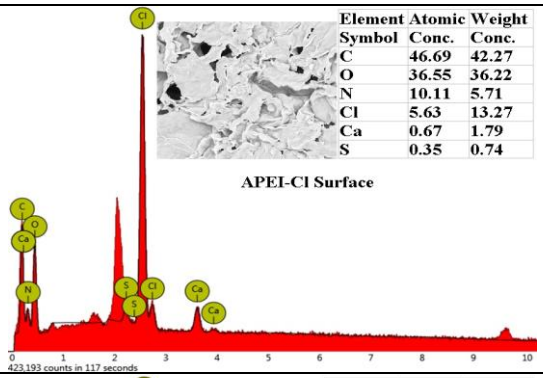
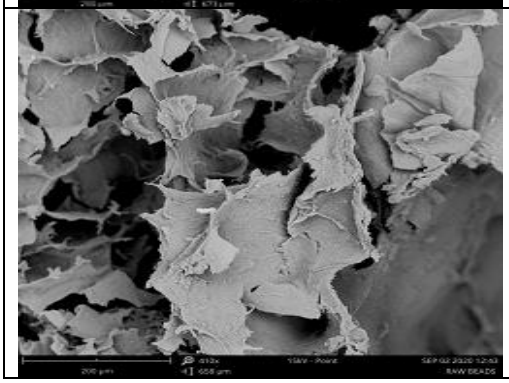	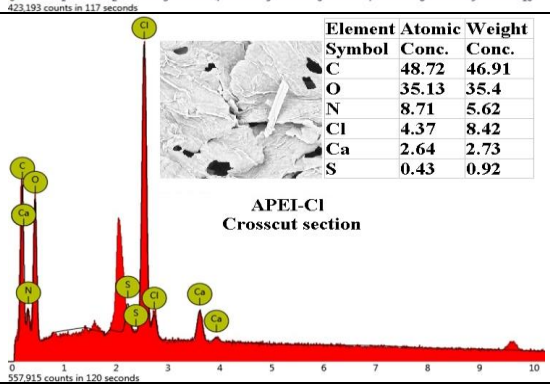

Table S2c. SEM-EDX of sorbent after grafting of phosphoryl groups (bar: 200 µm).

SEM	EDX
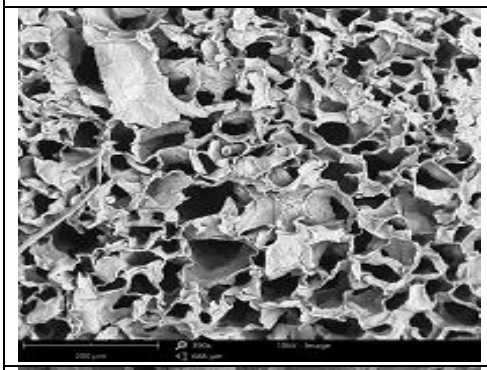	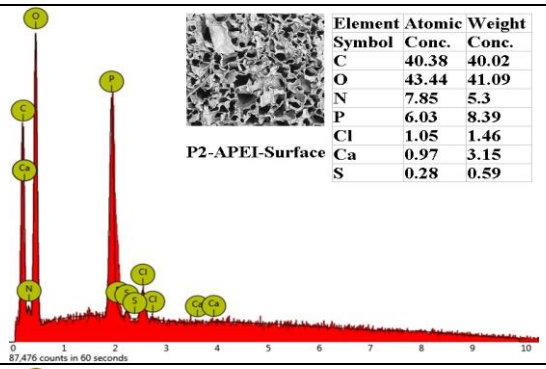 P2-APEI-Surface Element Symbol / Atomic Conc. / Weight Conc. C 40.38 40.02 O 43.44 41.09 N 7.85 5.3 P 6.03 8.39 Cl 1.05 1.46 Ca 0.97 3.15 S 0.28 0.59
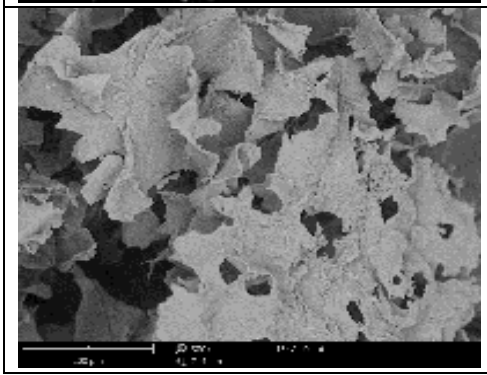	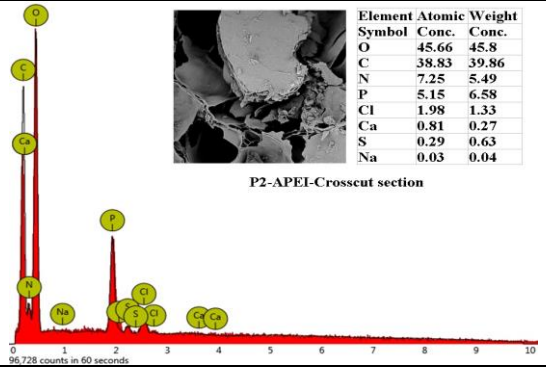 P2-APEI-Crosscut section Element Symbol / Atomic Conc. / Weight Conc. O 45.66 45.8 C 38.83 39.86 N 7.25 5.49 P 5.15 6.58 Cl 1.98 1.33 Ca 0.81 0.27 S 0.29 0.63 Na 0.03 0.04

Table S3. FTIR assignments and wavenumber (cm^{-1}) of APEI, APEI-Cl, and P2-APEI beads

Vibration	Ref.	Wn. in ref.	APEI	APEI-Cl	P2-APEI
O-H and N-H stretch (overlapped)	[7]	3500 -3000	3427	3423	3406
C-H aliphatic (stretch)	[7, 8]	2970-2950	2897	2935	2960
C(=O)O ester (stretch)	[8]	1750-1725			1741
C=O amide (stretch)	[9, 10]	1690-1630	1629, 1517	1627	1633
(-C=N-)/ 1° and 2° amine bending (overlapped)	[9, 10]	1690–1550		1519	1519
C-H bending	[9, 11-13]	1485–1430	1467	1467	1463
$-COO^-$ Salt	[9]	1420–1300	1384	1386	1384
1°/2° hydroxyl bending in-plane	[9]	1350–1260	1263	1259	
P=O (asymmetric)	[14-17]	1350-1250			1251
P(O) Phosphate ion (stretch)	[14-18]	1000-1100		1089	1033
C-C (stretch)	[19]	1350–1000	1095		
C-O-C, C-O (stretch)	[9]	1150-1050			
C-N (stretch)	[7, 8, 20-22]	1090-1020	1033	1035	
OH out-of-plane (bend)	[8, 9]	750–590	590	590	586
CH_2-Cl	[23]	700-800		788	
P-O-C (stretch)	[14-18]	570/990–1100			611/746

Table S4. FTIR assignments and wavenumber (cm^{-1}) of P2-APEI, loaded sorbent with either Pr(III) and Tm(III), and after 5 cycles of sorption and desorption.

Assignments	Ref.	Wn. in ref.	P-APEI	Pr(III)		Tm(III)	
				loaded	5 cycles	loaded	5 cycles
O-H and N-H stretch (overlapped)	[7]	3500 -3000	3406	3420	3411	3421	3412
C-H aliphatic (stretch)	[7, 8]	2970-2950	2960	2937	2947	2929	2933
C(=O)O ester (stretch)	[8]	1750-1725	1741	1627	1728	1627	1737
C=O amide (stretch)	[9, 10]	1690-1630	1633		1633		1633
(-C=N-)/ 1° and 2° amine bending (overlapped)	[9, 10]	1690–1550	1519				
C-H bending	[9, 11-13]	1485–1430	1463	1452 1404	1444	1452 1408	1452
$-COO^-$ Salt	[9]	1420–1300	1384		1388		1384
1°/2° hydroxyl bending in-plane	[9]	1350–1260					
P=O (asymmetric)	[14-17]	1250–1350	1251	1253	1251	1249	1255
P(O) Phosphate ion (stretch)	[14-18]	1000-1100	1033	1103	1035	1111	1035
C-N (stretch)	[7, 8, 20-22]	1090-1020					
C-O-C, C-O (stretch)	[9]	1150-1050		1037		1035	
C-C (stretch)	[19]	1350–1000					
P-O-C (stretch)	[14-18]	570/990–1100	611/746	545/808	561/812	536	611/810
Sulfate ion	[9]	680–610		617		617	
OH out-of-plane (bend)	[8, 9]	750–590	586				559

Table S5a. C 1s signal for APEI, P2-APEI (before and after metal sorption).

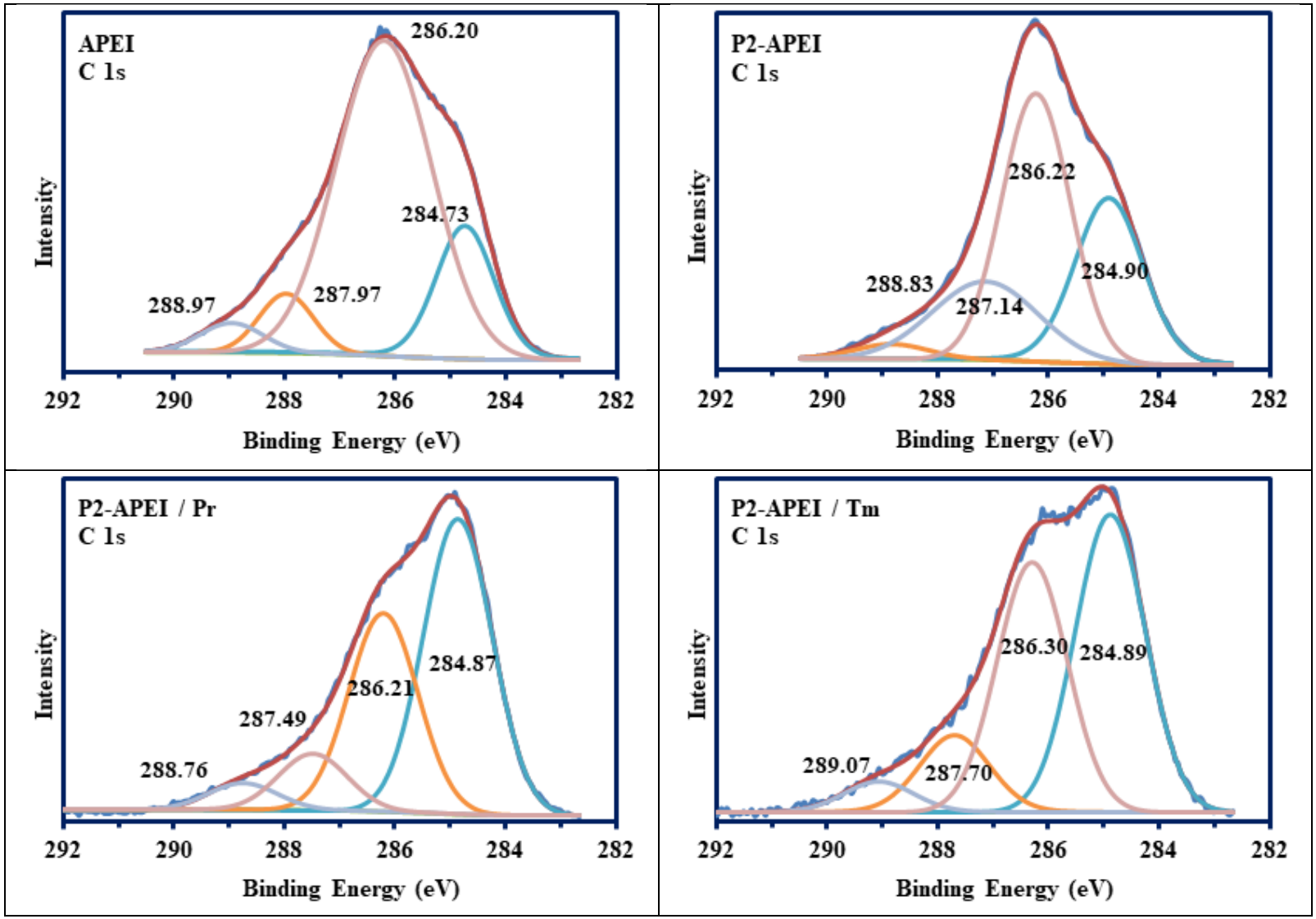

Table S5b. O 1s signal for APEI, P2-APEI (before and after metal sorption).

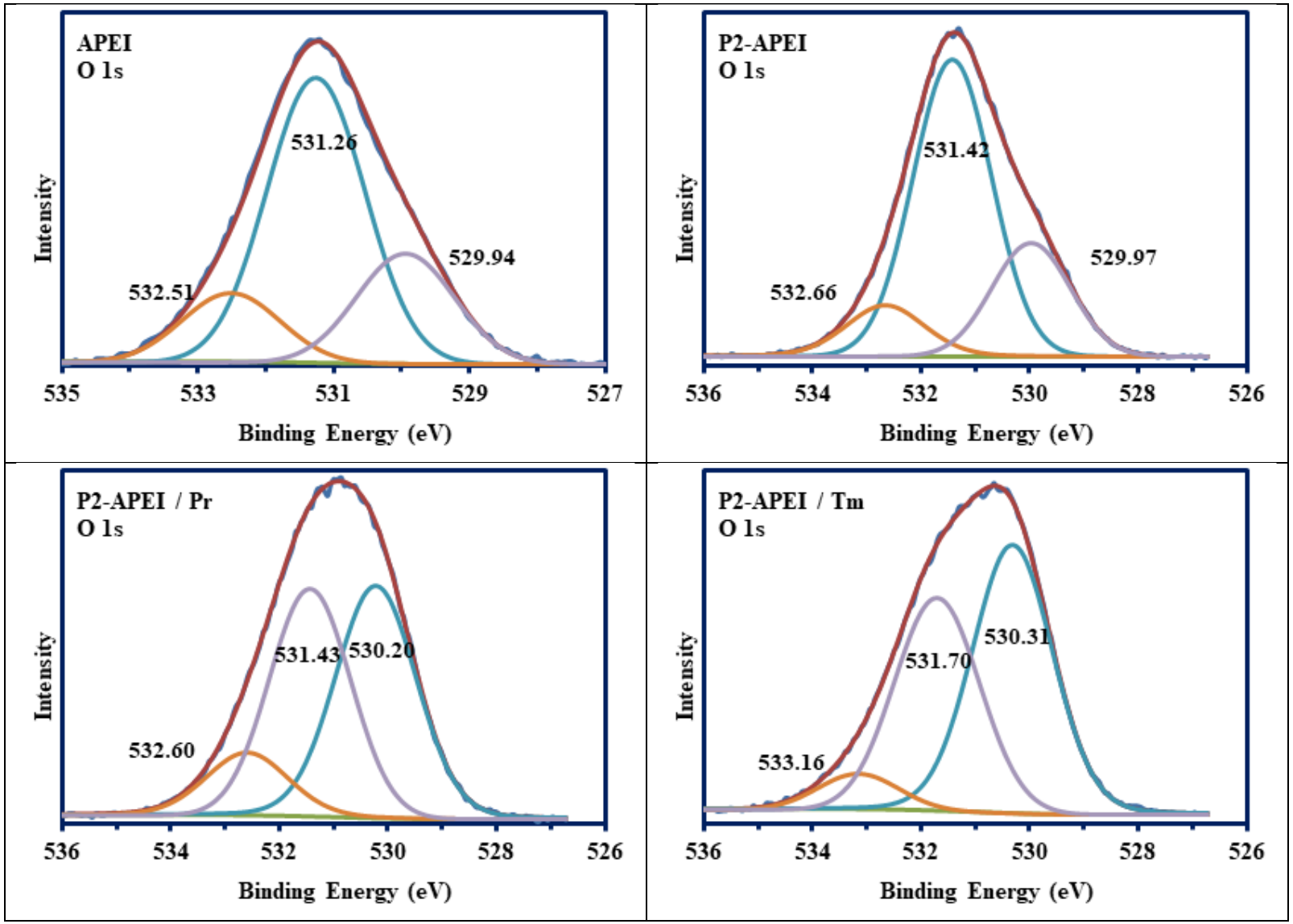

Table S5c. N 1s signal for APEI, P2-APEI (before and after metal sorption).

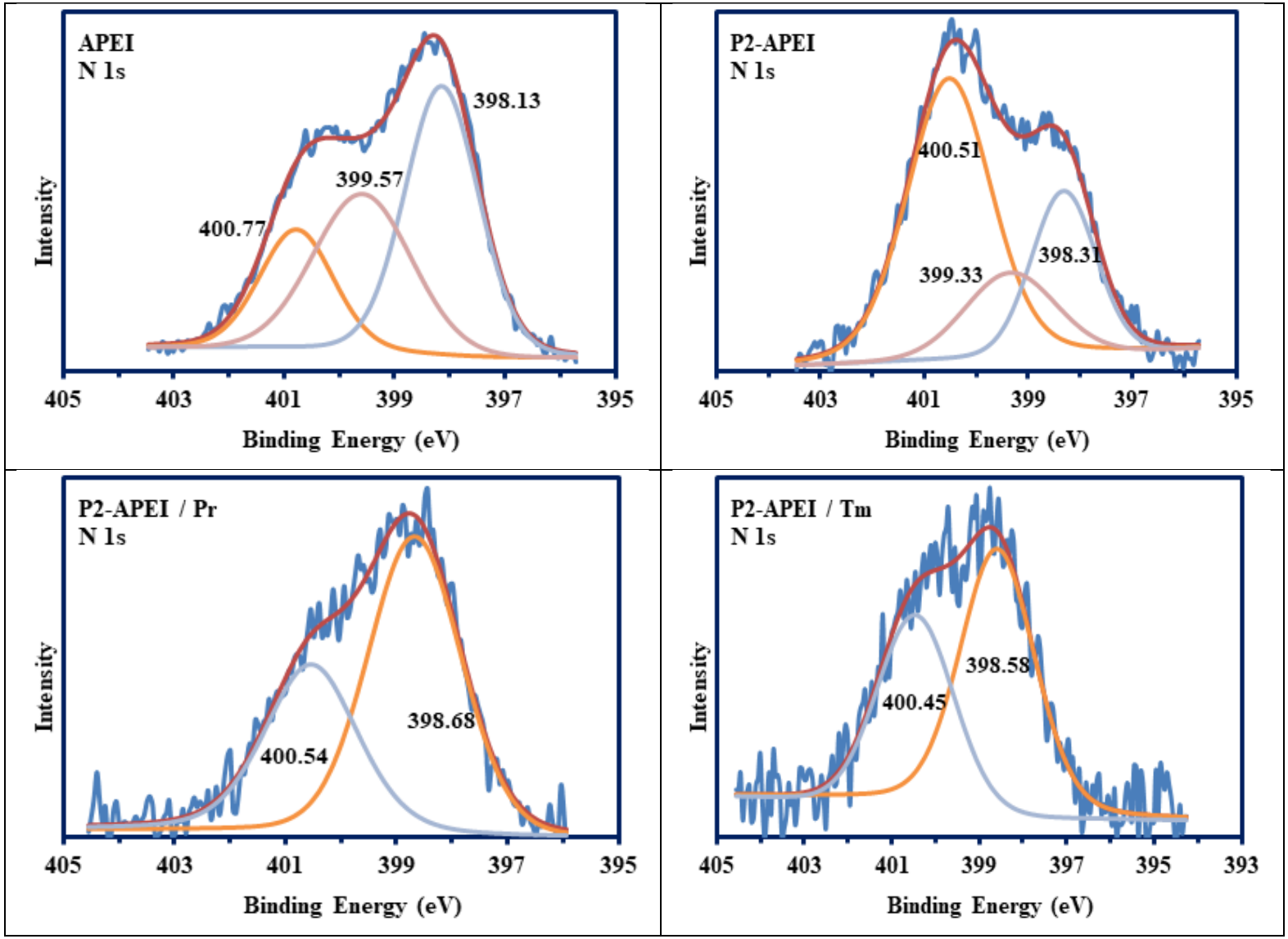

Table S5d. P 2p signal for APEI, P2-APEI (before and after metal sorption).

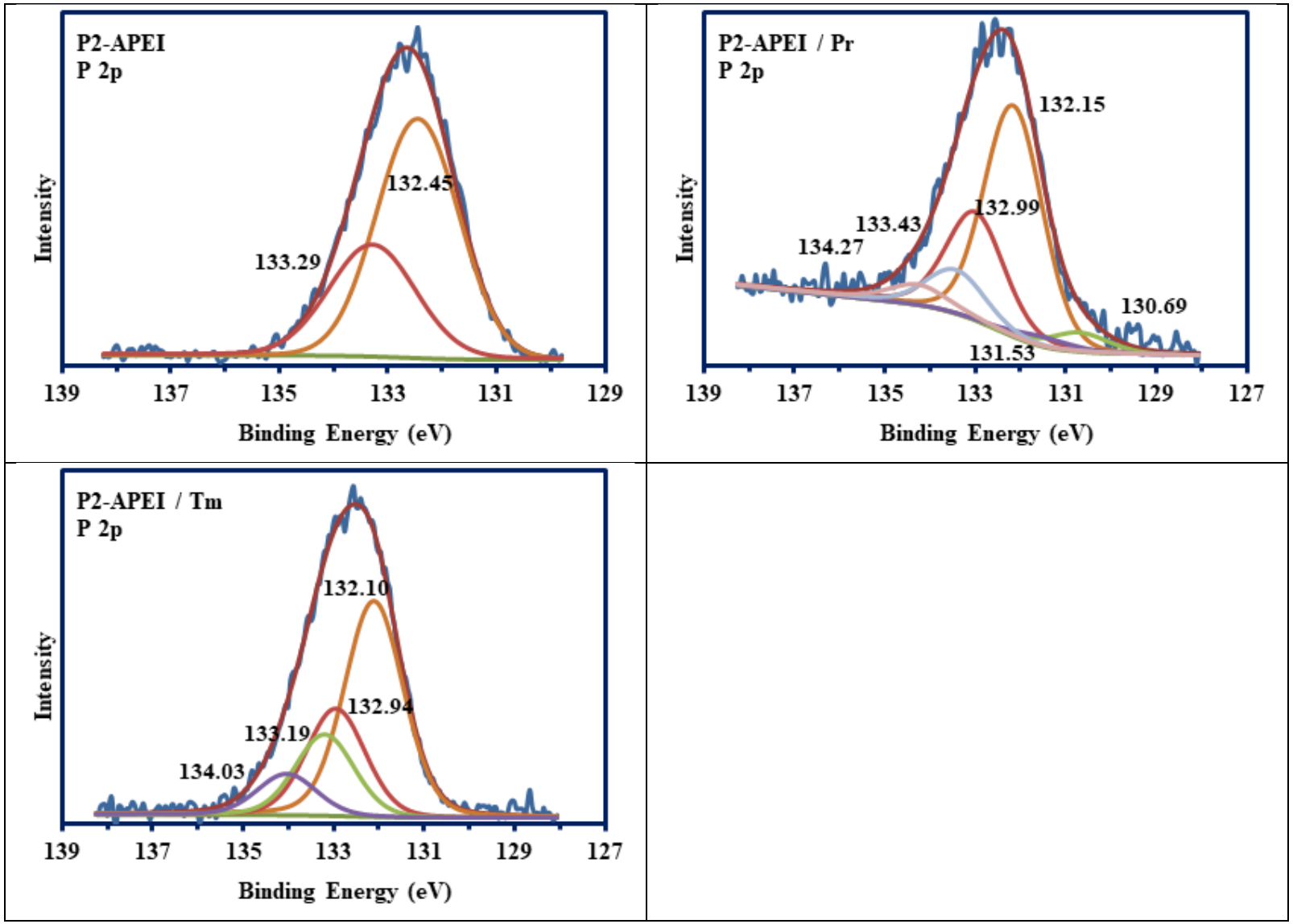

Table S5e. XPS signals, assignments and atomic fraction (AF) for APEI, P2-APEI (before & after metal sorption).

Signal	APEI	P2-APEI	P2-APEI + Pr(III)	P2-APEI + Tm(III)	Assignment
C 1s	284.73 (18.57)	284.90 (30.02)	284.87 (51.29)	284.89 (45.10)	C-C
	286.20 (69.80)	286.22 (46.39)	286.21 (34.39)	286.30 (37.74)	C-O-C, C-N
	287.97 (7.38)	287.14 (20.97)	287.49 (9.70)	287.70 (12.30)	C=O
	288.97 (4.25)	288.83 (2.62)	288.76 (4.63)	289.07 (4.85)	O-C=O, N-C=O
O 1s	529.94 (23.58)	529.97 (24.14)	530.22 (44.85)	530.31 (51.88)	OH
	531.26 (61.44)	531.42 (63.92)	531.43 (42.28)	531.70 (41.41)	C=O
	532.51 (14.98)	532.66 (11.94)	532.60 (12.87)	533.16 (6.71)	C-O-C, COOH
N 1s	398.13 (45.42)	398.31 (23.98)	398.68 (62.27)	398.58 (60.52)	R=N-R
	399.57 (34.20)	399.33 (17.51)			N-C=O, N-H, N-C
	400.77 (20.38)	400.51 (58.51)	400.54 (37.73)	400.45 (39.48)	N-(C=O)-O-(C=O)-N-(C=O)
P 2p			130.69 (4.63)		P $2p_{1/2}$
			131.53 (2.31)		P $2p_{3/2}$
		132.45 (66.67)	132.15 (52.06)	132.10 (48.32)	P-O-C, P-C, PO_3 (P $2p_{3/2}$)
			132.99 (26.03)	132.94 (24.16)	PO_4 (P $2p_{3/2}$)
		133.29 (33.33)	133.43 (9.97)	133.19 (18.35)	P-O-C, P-C, PO_3 (P $2p_{1/2}$)
			134.27 (4.99)	134.03 (9.17)	PO_4 (P $2p_{1/2}$)
S 2p	162.80 (17.38)	162.22 (10.55)	162.83 (13.26)	162.86 (18.40)	S $2p_{3/2}$ (R-SH)
	163.98 (8.69)	163.40 (5.27)	164.01 (6.63)	164.04 (9.20)	S $2p_{1/2}$ (R-SH)
	167.09 (49.29)	166.98 (56.12)	167.07 (46.07)	166.92 (48.26)	S $2p_{3/2}$ (sulfate)
	168.57 (24.64)	168.16 (28.06)	168.25 (23.04)	168.10 24.13)	S $2p_{1/2}$ (sulfate)
			168.66 (7.34)		S $2p_{3/2}$ (metal sulfate)
			169.84 (3.67)		S $2p_{1/2}$ (metal sulfate)
Cl 2p	196.28 (48.61)	196.21 (14.73)			Cl $2p_{3/2}$ (inorganic)
	197.70 (18.06)	197.81 (7.37)			Cl $2p_{3/2}$ (organic)
	197.88 (24.30)	198.82 (51.94)			Cl $2p_{1/2}$ (inorganic)
	199.30 (9.03)	200.42 (25.97)			Cl $2p_{1/2}$ (organic)
Ca 2p	346.26 (66.67)				Ca $2p_{3/2}$
	349.86 (33.33)				Ca $2p_{3/2}$

Table S6. Elemental analysis of APEI and P2-APEI sorbents.

Sorbent	C (%)	N (%)	N (mmol N g^{-1})	H (%)	O (%)	S (%)	P (%)	P (mmol P g^{-1})
APEI	39.43	5.85	4.18	6.98	35.01	0.41	0.001	-
P2-APEI	40.46	3.87	2.76	7.25	40.2	0.03	7.99	2.58

Table S7a. SEM-EDX of raw beads (APEI) before and after loading with Pr(III) and Tm(III) (surface and crosscut section) at pH_0 5

SEM	EDX
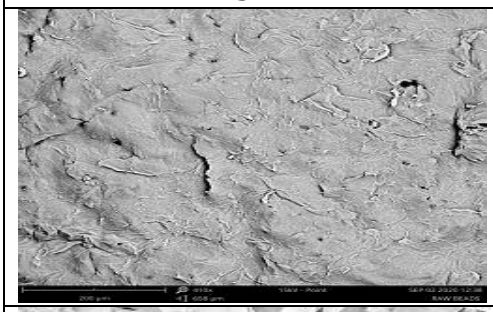	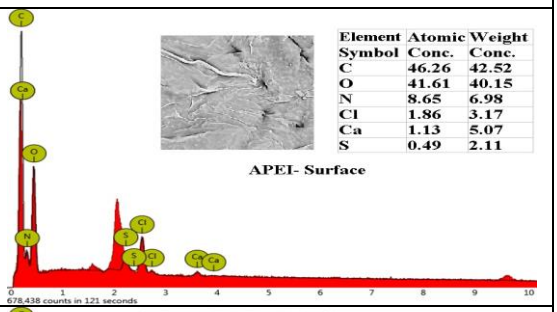
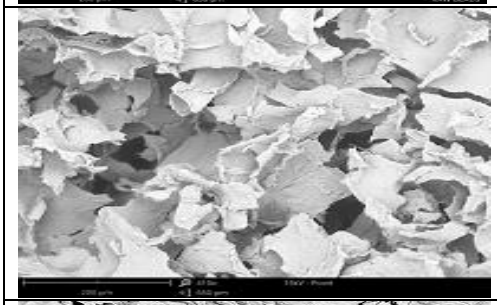	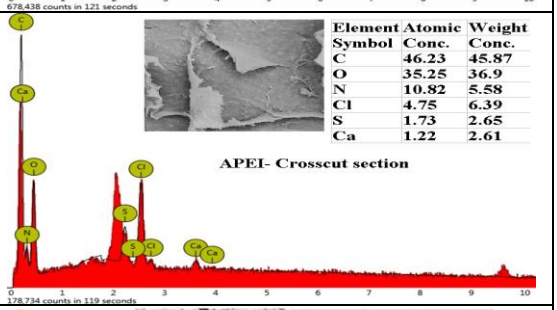
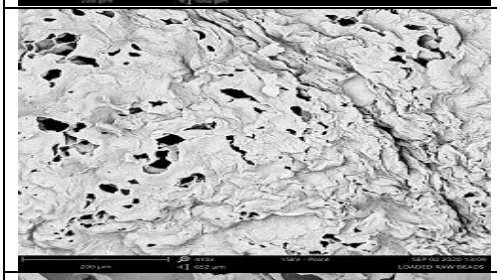	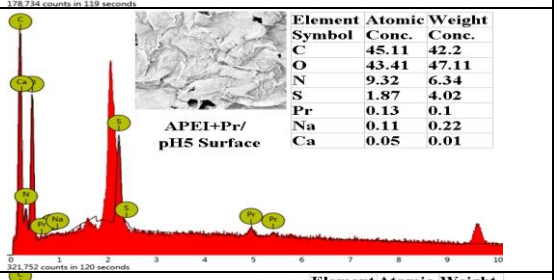
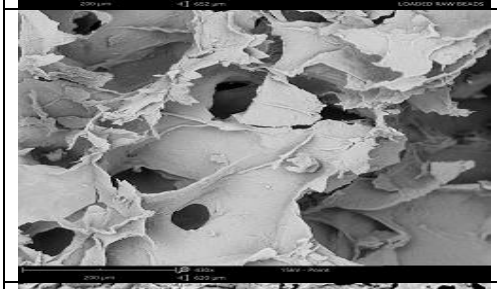	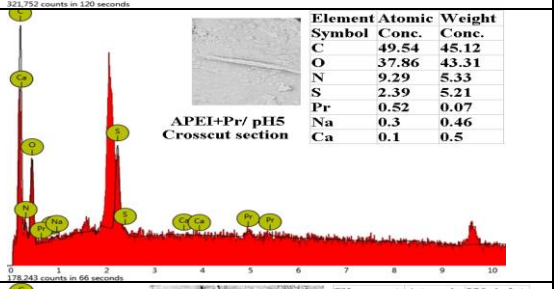
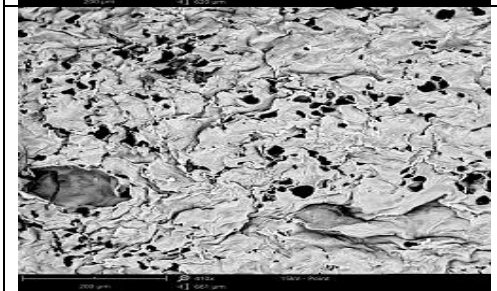	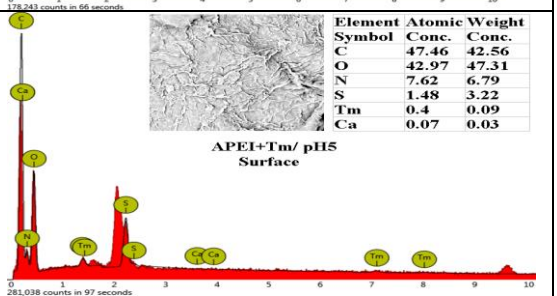
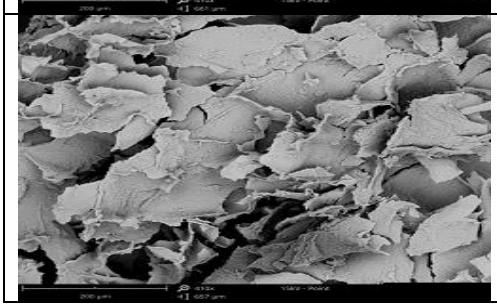	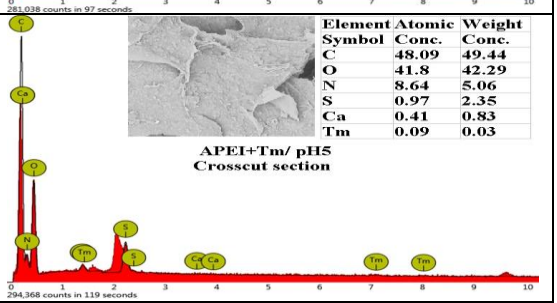

Table S7b. SEM-EDX of loaded P2-APEI sorbent (surface and crosscut section)

SEM	EDX
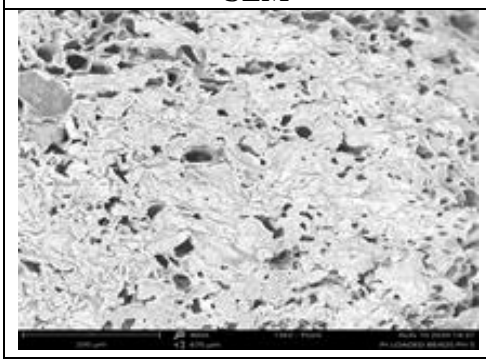	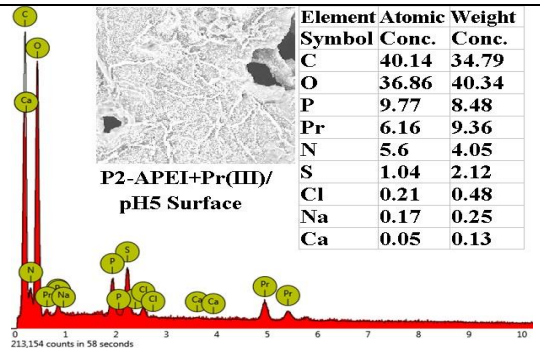 Element Symbol / Atomic Conc. / Weight Conc. C 40.14 34.79 O 36.86 40.34 P 9.77 8.48 Pr 6.16 9.36 N 5.6 4.05 S 1.04 2.12 Cl 0.21 0.48 Na 0.17 0.25 Ca 0.05 0.13
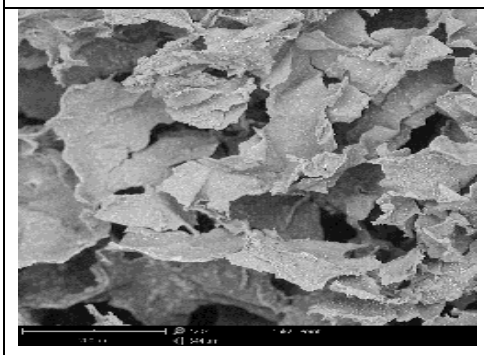	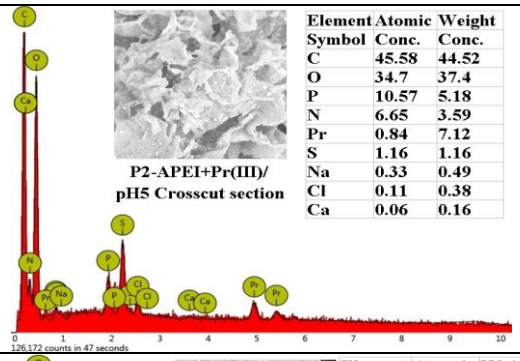 Element Symbol / Atomic Conc. / Weight Conc. C 45.58 44.52 O 34.7 37.4 P 10.57 5.18 N 6.65 3.59 Pr 0.84 7.12 S 1.16 1.16 Na 0.33 0.49 Cl 0.11 0.38 Ca 0.06 0.16
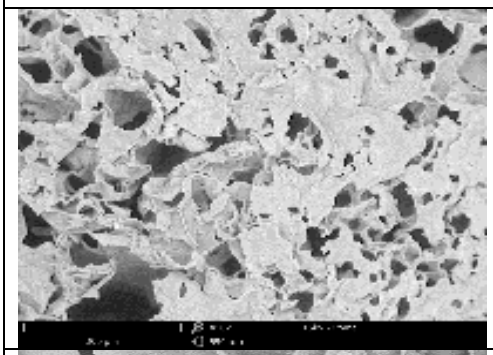	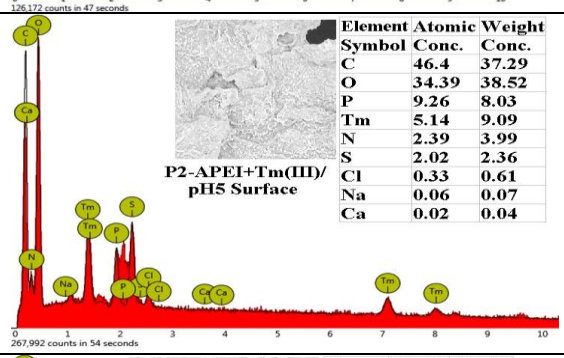 Element Symbol / Atomic Conc. / Weight Conc. C 46.4 37.29 O 34.39 38.52 P 9.26 8.03 Tm 5.14 9.09 N 2.39 3.99 S 2.02 2.36 Cl 0.33 0.61 Na 0.06 0.07 Ca 0.02 0.04
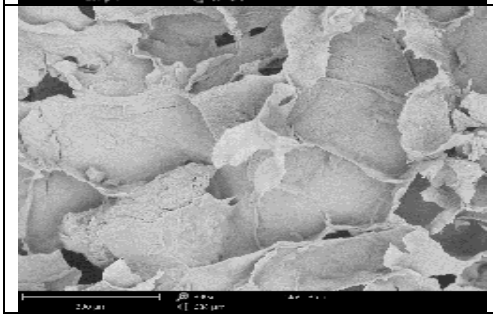	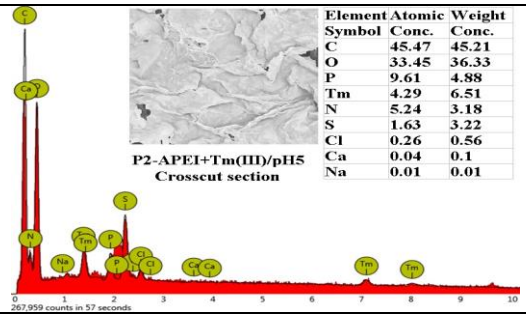 Element Symbol / Atomic Conc. / Weight Conc. C 45.47 45.21 O 33.45 36.33 P 9.61 4.88 Tm 4.29 6.51 N 5.24 3.18 S 1.63 3.22 Cl 0.26 0.56 Ca 0.04 0.1 Na 0.01 0.01

Table S7c. SEM-EDX of P2-APEI sorbent after elution (surface and crosscut section)

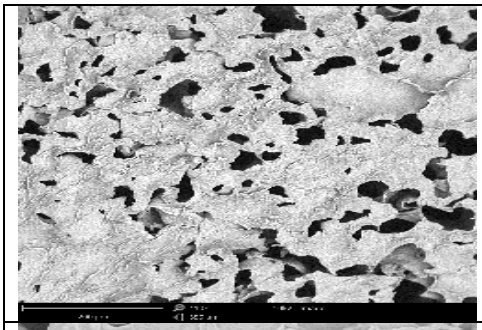

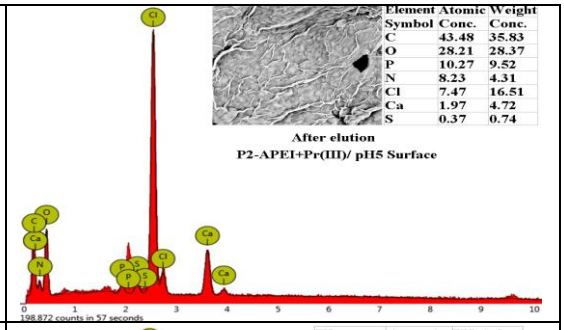
Element Symbol
Atomic Conc.
Weight Conc.
C 43.48 35.83
O 28.21 28.37
P 10.27 9.52
N 8.23 4.31
Cl 7.47 16.51
Ca 1.97 4.72
S 0.37 0.74
After elution
P2-APEI+Pr(III)/ pH5 Surface
198,872 counts in 57 seconds

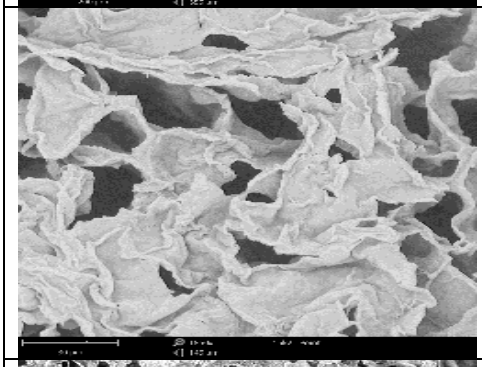

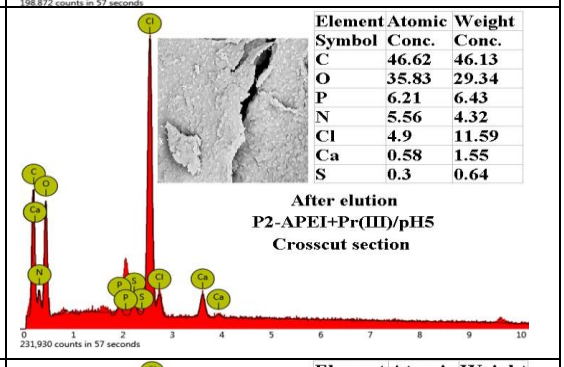
Element Symbol
Atomic Conc.
Weight Conc.
C 46.62 46.13
O 35.83 29.34
P 6.21 6.43
N 5.56 4.32
Cl 4.9 11.59
Ca 0.58 1.55
S 0.3 0.64
After elution
P2-APEI+Pr(III)/pH5
Crosscut section
231,930 counts in 57 seconds

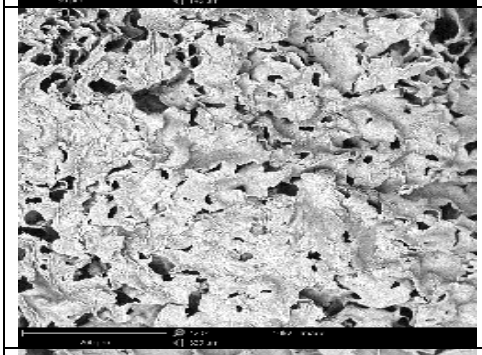

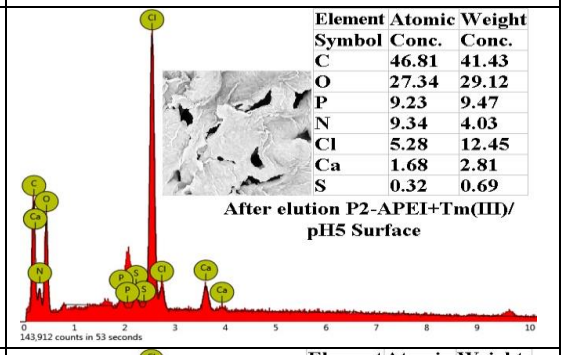
Element Symbol
Atomic Conc.
Weight Conc.
C 46.81 41.43
O 27.34 29.12
P 9.23 9.47
N 9.34 4.03
Cl 5.28 12.45
Ca 1.68 2.81
S 0.32 0.69
After elution P2-APEI+Tm(III)/
pH5 Surface
143,912 counts in 53 seconds

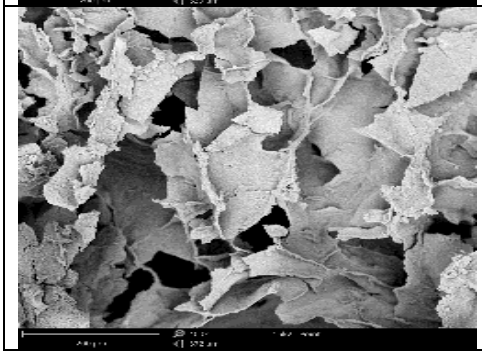

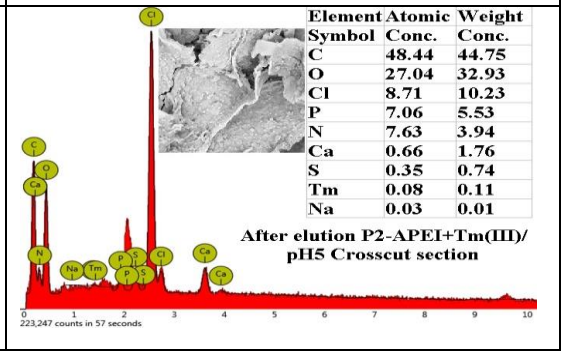
Element Symbol
Atomic Conc.
Weight Conc.
C 48.44 44.75
O 27.04 32.93
Cl 8.71 10.23
P 7.06 5.53
N 7.63 3.94
Ca 0.66 1.76
S 0.35 0.74
Tm 0.08 0.11
Na 0.03 0.01
After elution P2-APEI+Tm(III)/
pH5 Crosscut section
223,247 counts in 57 seconds

Table S8. SEM-EDX analysis of P2-APEI after treated with equimolar solution at different pH values.

Surface	Crosscut section
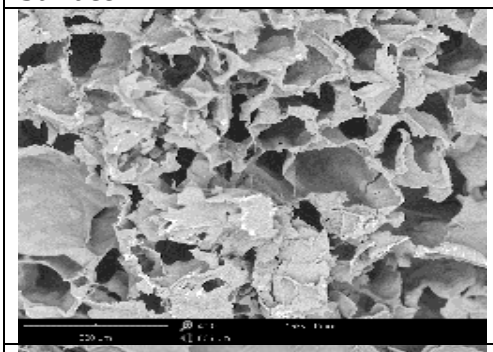	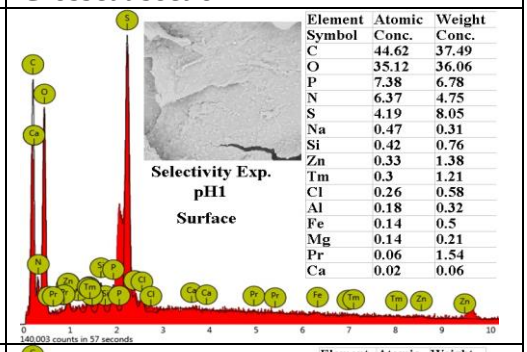
	Element Symbol / Atomic Conc. / Weight Conc. C 44.62 37.49 O 35.12 36.06 P 7.38 6.78 N 6.37 4.75 S 4.19 8.05 Na 0.47 0.31 Si 0.42 0.76 Zn 0.33 1.38 Tm 0.3 1.21 Cl 0.26 0.58 Al 0.18 0.32 Fe 0.14 0.5 Mg 0.14 0.21 Pr 0.06 1.54 Ca 0.02 0.06
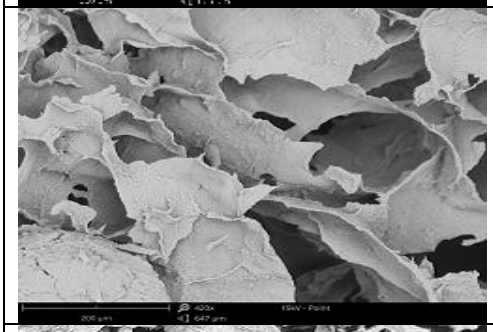	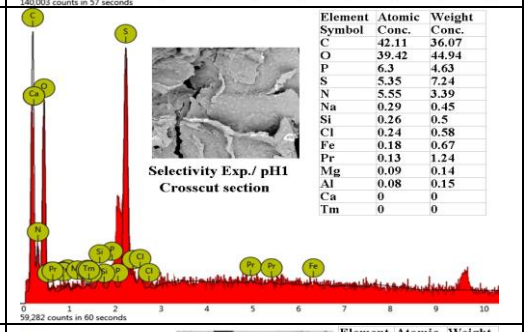
	Element Symbol / Atomic Conc. / Weight Conc. C 42.11 36.07 O 39.42 44.94 P 6.3 4.63 S 5.35 7.24 N 5.55 3.39 Na 0.29 0.45 Si 0.26 0.5 Cl 0.24 0.58 Fe 0.18 0.67 Pr 0.13 1.24 Mg 0.09 0.14 Al 0.08 0.15 Ca 0 0 Tm 0 0
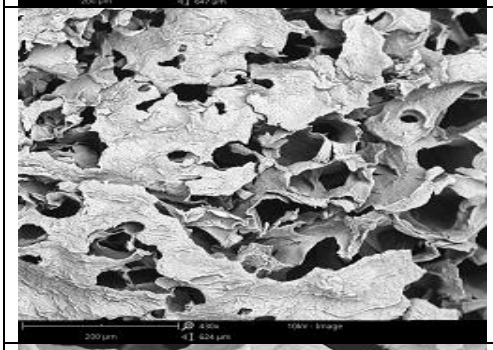	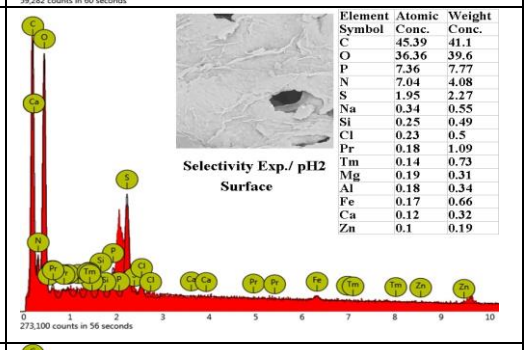
	Element Symbol / Atomic Conc. / Weight Conc. C 45.39 41.1 O 36.36 39.6 P 7.36 7.77 N 7.04 4.08 S 1.95 2.27 Na 0.34 0.55 Si 0.25 0.49 Cl 0.23 0.5 Pr 0.18 1.09 Tm 0.14 0.73 Mg 0.19 0.31 Al 0.18 0.34 Fe 0.17 0.66 Ca 0.12 0.32 Zn 0.1 0.19
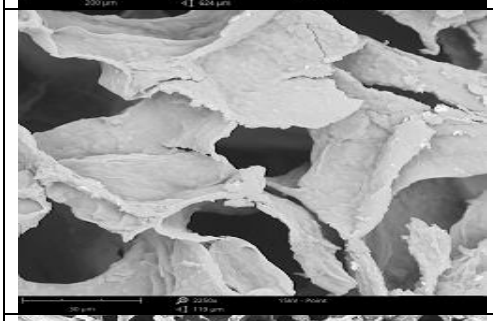	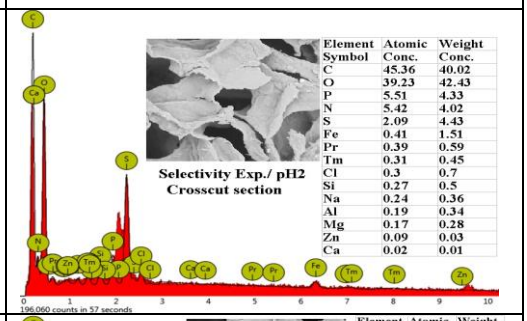
	Element Symbol / Atomic Conc. / Weight Conc. C 45.36 40.02 O 39.23 42.43 P 5.51 4.33 N 5.42 4.02 S 2.09 4.43 Fe 0.41 1.51 Pr 0.39 0.59 Tm 0.31 0.45 Cl 0.3 0.7 Si 0.27 0.5 Na 0.24 0.36 Al 0.19 0.34 Mg 0.17 0.28 Zn 0.09 0.03 Ca 0.02 0.01
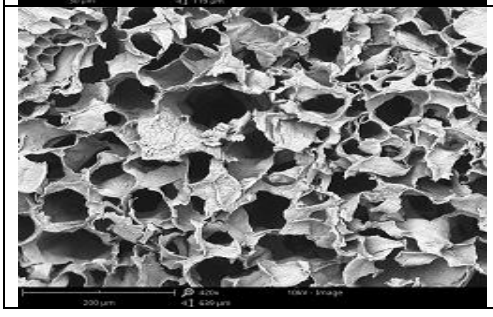	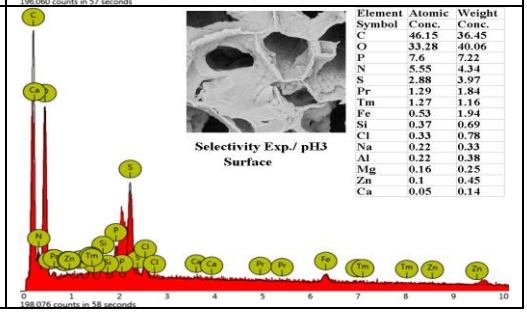
	Element Symbol / Atomic Conc. / Weight Conc. C 46.15 36.45 O 33.28 40.06 P 7.6 7.22 N 5.55 4.34 S 2.88 3.97 Pr 1.29 1.84 Tm 1.27 1.16 Fe 0.53 1.94 Si 0.37 0.69 Cl 0.33 0.78 Na 0.22 0.33 Al 0.22 0.38 Mg 0.16 0.25 Zn 0.1 0.45 Ca 0.05 0.14

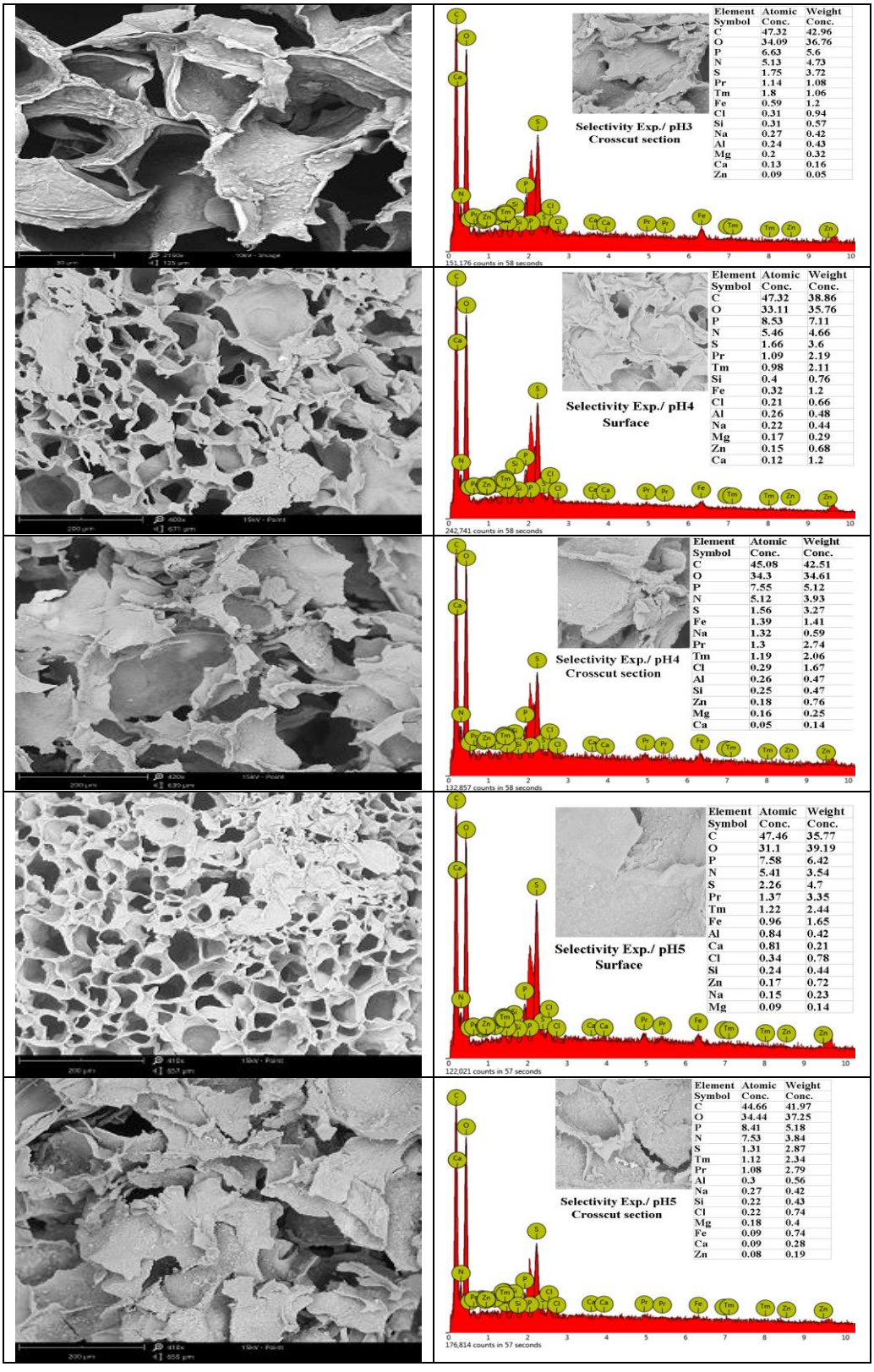
Selectivity Exp./ pH3
Crosscut section
Element Symbol | Atomic Conc. | Weight Conc.
C | 47.32 | 42.96
O | 34.09 | 36.76
P | 6.63 | 5.6
N | 5.13 | 4.73
S | 1.75 | 3.72
Pr | 1.14 | 1.08
Tm | 1.8 | 1.06
Fe | 0.59 | 1.2
Cl | 0.31 | 0.94
Si | 0.31 | 0.57
Na | 0.27 | 0.42
Al | 0.24 | 0.43
Mg | 0.2 | 0.32
Ca | 0.13 | 0.16
Zn | 0.09 | 0.05
151,176 counts in 58 seconds
Selectivity Exp./ pH4
Surface
Element Symbol | Atomic Conc. | Weight Conc.
C | 47.32 | 38.86
O | 33.11 | 35.76
P | 8.53 | 7.11
N | 5.46 | 4.66
S | 1.66 | 3.6
Pr | 1.09 | 2.19
Tm | 0.98 | 2.11
Si | 0.4 | 0.76
Fe | 0.32 | 1.2
Cl | 0.21 | 0.66
Al | 0.26 | 0.48
Na | 0.22 | 0.44
Mg | 0.17 | 0.29
Zn | 0.15 | 0.68
Ca | 0.12 | 1.2
242,741 counts in 58 seconds
Selectivity Exp./ pH4
Crosscut section
Element Symbol | Atomic Conc. | Weight Conc.
C | 45.08 | 42.51
O | 34.3 | 34.61
P | 7.55 | 5.12
N | 5.12 | 3.93
S | 1.56 | 3.27
Fe | 1.39 | 1.41
Na | 1.32 | 0.59
Pr | 1.3 | 2.74
Tm | 1.19 | 2.06
Cl | 0.29 | 1.67
Al | 0.26 | 0.47
Si | 0.25 | 0.47
Zn | 0.18 | 0.76
Mg | 0.16 | 0.25
Ca | 0.05 | 0.14
132,857 counts in 58 seconds
Selectivity Exp./ pH5
Surface
Element Symbol | Atomic Conc. | Weight Conc.
C | 47.46 | 35.77
O | 31.1 | 39.19
P | 7.58 | 6.42
N | 5.41 | 3.54
S | 2.26 | 4.7
Pr | 1.37 | 3.35
Tm | 1.22 | 2.44
Fe | 0.96 | 1.65
Al | 0.84 | 0.42
Ca | 0.81 | 0.21
Cl | 0.34 | 0.78
Si | 0.24 | 0.44
Zn | 0.17 | 0.72
Na | 0.15 | 0.23
Mg | 0.09 | 0.14
122,021 counts in 57 seconds
Selectivity Exp./ pH5
Crosscut section
Element Symbol | Atomic Conc. | Weight Conc.
C | 44.66 | 41.97
O | 34.44 | 37.25
P | 8.41 | 5.18
N | 7.53 | 3.84
S | 1.31 | 2.87
Tm | 1.12 | 2.34
Pr | 1.08 | 2.79
Al | 0.3 | 0.56
Na | 0.27 | 0.42
Si | 0.22 | 0.43
Cl | 0.22 | 0.74
Mg | 0.18 | 0.4
Fe | 0.09 | 0.74
Ca | 0.09 | 0.28
Zn | 0.08 | 0.19
176,814 counts in 57 seconds

Table S9. Pr(III) and Tm(III) desorption kinetics using APEI and P2-APEI sorbents from binary solutions – Fitting parameters for PFORE and PSORE models.

Model	Parameter	Sorbent			
		APEI		P2-APEI	
		Pr(III)	Tm(III)	Pr(III)	Tm(III)
Exp.	$q_{eq,exp}$ (mmol g^{-1})	0.0461	0.0450	0.191	0.184
PFORE	$q_{1,calc}$ (mmol g^{-1})	0.0461	0.0456	0.230	0.357
	$k_1 \times 10$ (min^{-1})	2.27	1.31	0.612	0.246
	R^2	0.987	0.975	0.990	0.990
	AIC	-94	-89	-72	-74
PSORE	$q_{2,calc}$ (mmol g^{-1})	0.0532	0.0562	0.334	0.616
	k_2 (L $mmol^{-1}$ min^{-1})	5.43	2.51	0.140	0.024
	R^2	0.991	0.984	0.990	0.990
	AIC	-98	-93	-74	-74

Table S10. Composition of ore and tailing – Main elements

Element (oxide)	Ore Conc. (%)	Tailing Conc. (%)	Element	Ore Conc. (mg g^{-1})	Tailing Conc. (mg g^{-1})
SiO_2	36.76	35.29	U	1033	294
Al_2O_3	12.01	4.54	Cu	4020	816
Fe_2O_3	9.85	4.13	Ni	210	105
CaO	8.96	4.21	V	189	19
Na_2O	2.01	0.19	REE	794	227
MgO	7.44	2.69	Mo	201	85
K_2O	1.96	0.16	Zn	518	77
MnO	1.18	0.58	Co	32	14
*L.O.I.	18.81	22.33			

*L.O.I. loss on ignition (%).

Table S11. Composition of tailing leachate and after successive pre-treatments.

Metal ion	Leachate	Precipitation pH 4	Precipitation pH 5	Sorption				
				pH_{eq} 1.38	pH_{eq} 2.34	pH_{eq} 3.41	pH_{eq} 3.68	pH_{eq} 3.91
Si(IV)	58.93	55.68	54.97	54.19	53.90	53.29	52.34	51.88
Al(III)	2779	2537	84.04	83.01	82.77	80.87	77.16	76.11
Fe(III)	6804	89.18	26.48	26.28	25.17	23.50	23.22	23.19
Ca(II)	1875	1838	1833	1830	1814	1794	1773	1732
Mn(II)	106.0	103.5	98.91	98.05	97.67	95.49	94.39	93.90
Ni(II)	29.97	27.98	27.00	26.48	26.39	26.19	25.50	24.56
Cu(II)	188.9	183.2	182.9	181.9	176.8	174.2	172.4	170.2
Nd (III)	21.35	20.95	20.19	17.69	10.60	7.22	3.25	1.21
Pr(III)	15.76	15.31	15.20	13.59	8.06	5.86	2.28	0.99
Tm(II)	3.90	3.88	3.61	3.28	2.55	2.00	1.39	0.25
Zn(II)	12.96	11.39	11.00	10.96	10.56	10.09	9.40	8.22
REE(III)	97.50	95.89	94.89	82.90	62.05	37.90	28.77	14.90

Table S12. Distribution ratio (D, L g^{-1}) for the sorption of metals from pre-treated leachates (at different values of pH_{eq})

Element	pH 1.38	pH 2.34	pH 3.41	pH 3.68	pH 3.91
Si(IV)	14.48	19.71	31.59	50.30	59.30
Al(III)	12.31	15.20	39.08	89.11	103.68
Fe(III)	7.45	51.72	126.7	139.9	141.1
Ca(II)	1.40	10.56	21.49	33.67	58.33
Mn(II)	8.72	12.59	35.74	47.79	53.14
Ni(II)	19.55	22.87	30.81	58.80	98.67
Cu(II)	5.53	34.59	49.98	61.00	74.54
Zn(II)	3.69	40.94	89.94	169.3	337.3
Nd(III)	140.8	899	1794	5196	15573
Pr(III)	118.3	881.6	1595	5654	14294
Tm(III)	98.0	412.0	800.8	1593	13575

Table S13. SEM analysis of P2-APEI beads (surface and crosscut section) after sorption step onto pre-treated leachate of tailings.

	Surface	Crosscut section
pH 1	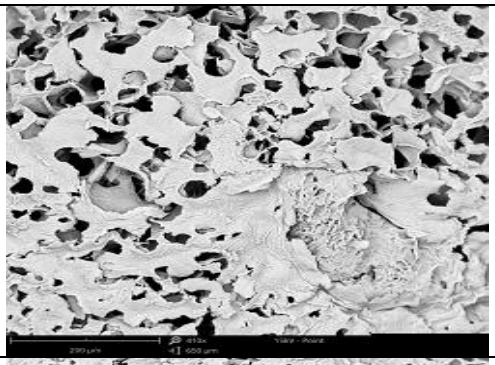	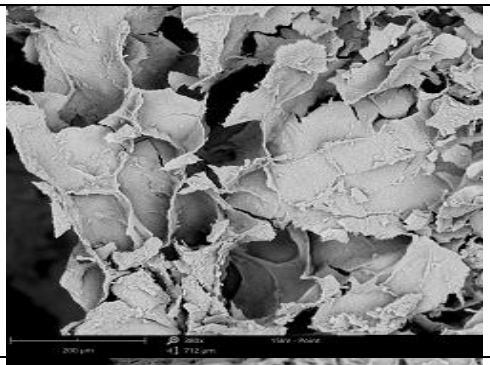
pH 2	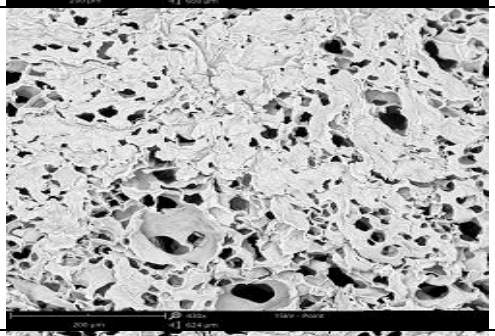	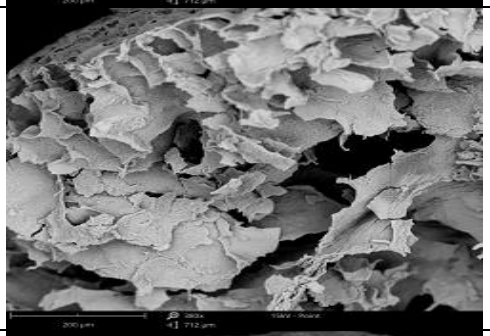
pH 3	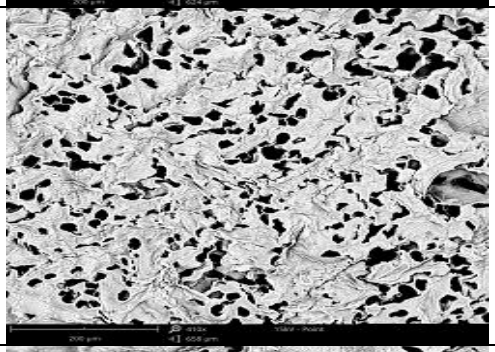	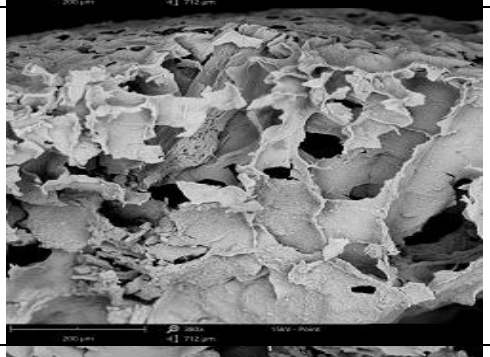
pH 4	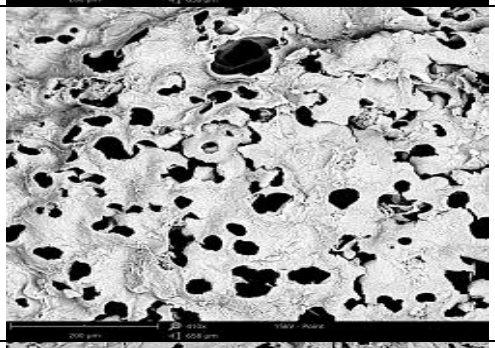	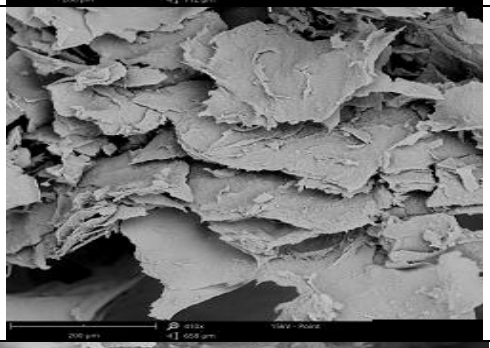
pH 5	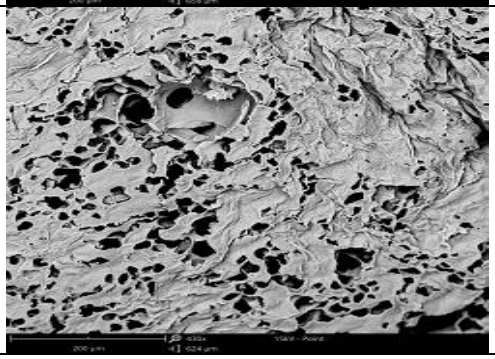	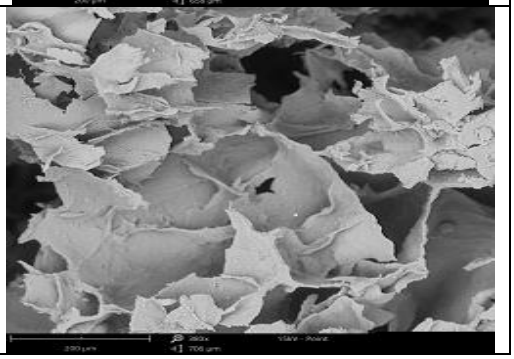

Table S14. EDX analysis of the sorbent (surface and crosscut section) after application at pH_0 5.

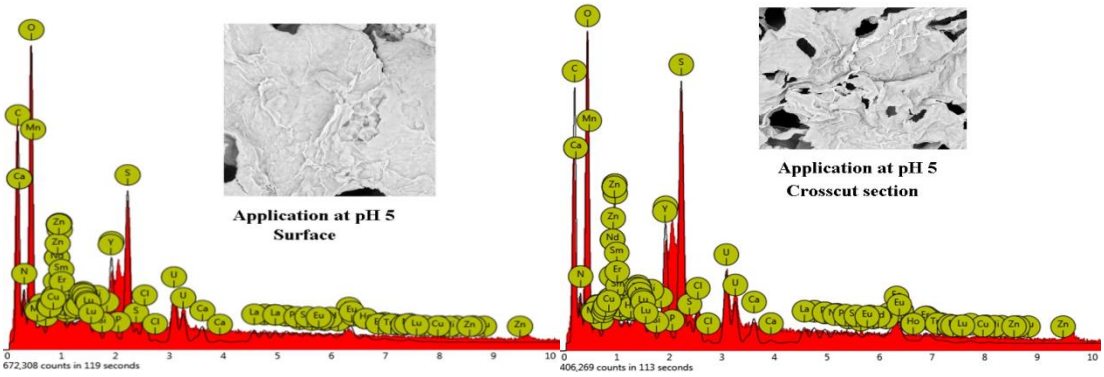

	Surface		Crosscut section	
Element	Atomic Fraction (%)	Weight Fraction (%)	Atomic Fraction (%)	Weight Fraction (%)
C	41.64	16.76	37.14	23.86
O	25.72	15.8	24.94	14.07
N	5.03	4.65	4.53	3.46
S	3.11	3.34	5.08	4.59
P	7.56	6.62	9.13	5.32
Cl	0.6	0.72	0.7	0.76
Na	2.42	1.87	3.34	2.32
Mg	0.6	0.49	0.59	1.44
Al	0.57	0.52	0.65	0.53
Si	0.63	0.59	0.71	0.61
Ca	0.35	0.47	0.52	0.63
Mn	0.11	0.21	0.31	0.51
Fe	0.74	1.38	1.15	1.95
Ni	0.17	0.33	0.15	0.26
Cu	0.42	0.9	0.49	0.94
Zn	0.46	1	0.48	0.95
Y	0.31	0.94	0.33	0.88
La	0.45	2.61	0.55	2.33
Ce	0.51	2.4	0.62	2.61
Pr	0.53	2.52	0.28	1.18
Nd	0.33	1.5	0.27	1.18
Pm	0.19	0.94	0.37	0.62
Sm	0.31	1.96	0.39	1.76
Eu	0.2	1	0.08	0.36
Gd	0.47	2.48	0.41	1.97
Tb	0.56	2.09	0.65	1.15
Dy	0.38	2.04	0.49	1.41
Ho	0.54	1.97	0.71	1.54
Er	0.45	2.52	0.6	1.02
Tm	0.63	1.55	0.68	1.47
Yb	0.5	2.92	0.59	2.08
Lu	0.97	2.66	0.96	1.08
U	2.54	12.25	2.11	15.16

Table S15. Metal concentrations (mg L^{-1}) in the eluate from sorbent loaded at different values of pH_{eq}.

Element	pH 1.38	pH 2.34	pH 3.41	pH 3.68	pH 3.91
Si(IV)	3.82	4.99	8.14	12.55	14.77
Al(III)	4.87	5.89	14.84	33.78	38.97
Fe(III)	0.88	6.33	14.66	15.73	16.09
Ca(II)	12.44	95.29	188.00	294.83	499.75
Mn(II)	3.99	5.89	16.66	22.22	24.03
Ni(II)	2.43	2.89	3.74	6.99	11.78
Cu(II)	4.79	28.88	42.80	51.79	63.29
Zn(II)	0.20	2.09	4.43	7.89	13.08
Nd(III)	12.22	47.05	63.89	83.99	93.89
Pr(III)	7.86	34.84	45.79	64.12	69.86
Tm(III)	1.60	5.19	7.90	10.79	16.16

Table S16. Metal concentrations (mg L^{-1}) in the residue of oxalic acid precipitation from eluates collected from sorbent loaded at different values of pH_{eq}.

Element	pH 1.38	pH 2.34	pH 3.41	pH 3.68	pH 3.91
Si(IV)	3.69	4.75	7.59	11.30	12.99
Al(III)	4.69	5.68	13.49	31.35	36.59
Fe(III)	0.75	5.70	13.49	14.48	15.49
Ca(II)	11.39	87.39	175.49	174.38	475.49
Mn(II)	3.74	5.49	15.23	21.04	21.03
Ni(II)	2.36	2.54	3.23	5.98	9.99
Cu(II)	3.97	25.91	38.49	49.39	57.27
Zn(II)	0.16	1.90	4.39	7.48	10.50
Nd(III)	11.49	45.68	58.89	1.39	1.46
Pr(III)	6.29	29.39	42.39	1.59	1.39
Tm(III)	1.39	4.61	7.40	0.40	0.30

Table S17. EDX analysis of the oxalate precipitate from sorbent loaded at pH_0 5

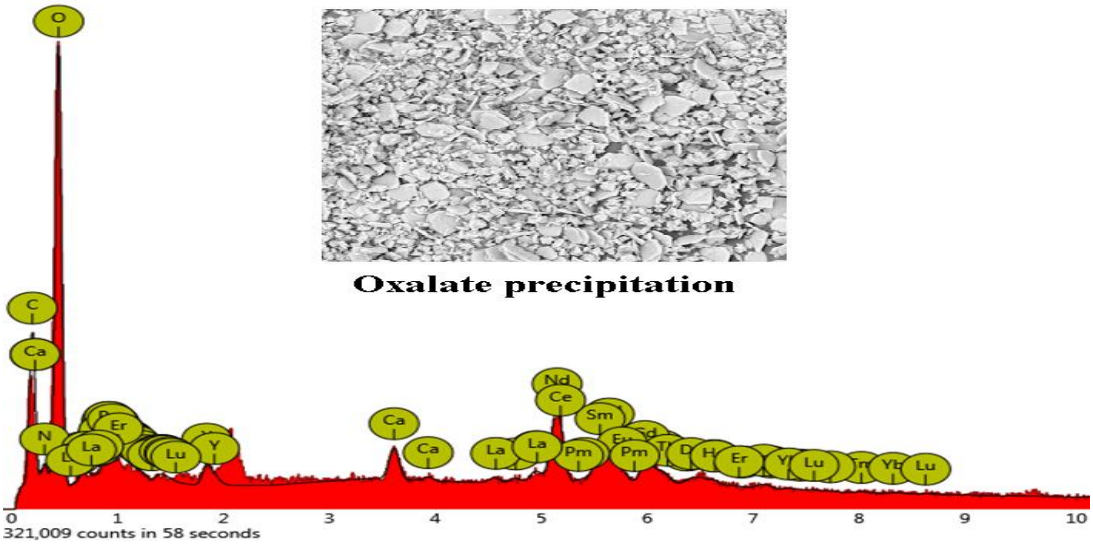

Element	Atomic fraction (%)	Weight fraction (%)
O	44.79	19.46
C	31.64	11.12
N	0.96	1.49
Ca	1.05	1.15
Y	2.23	2.0
La	0.21	0.78
Ce	0.38	1.44
Pr	0.95	2.87
Nd	5.58	21.83
Pm	0.18	0.71
Sm	3.62	10.82
Eu	1.71	3.64
Gd	2.57	6.68
Tb	0.55	2.38
Dy	1.24	3.71
Ho	0.4	1.8
Er	0.3	1.38
Tm	0.76	2.59
Yb	0.45	2.09
Lu	0.43	2.06

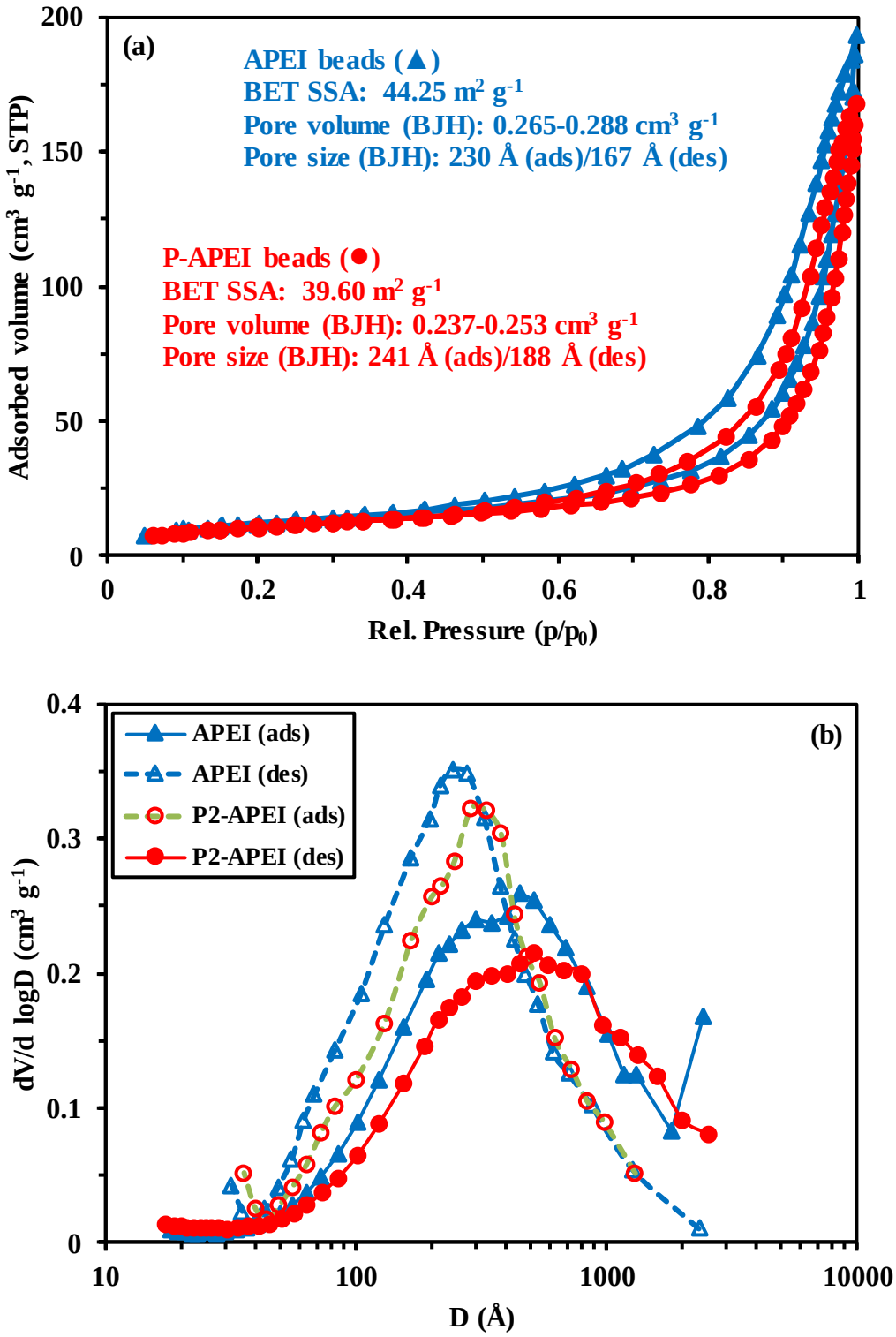

Figure S1. Textural analysis of APEI and P2-APEI sorbents – (a) S_{BET} surface area, (b) pore size distribution.

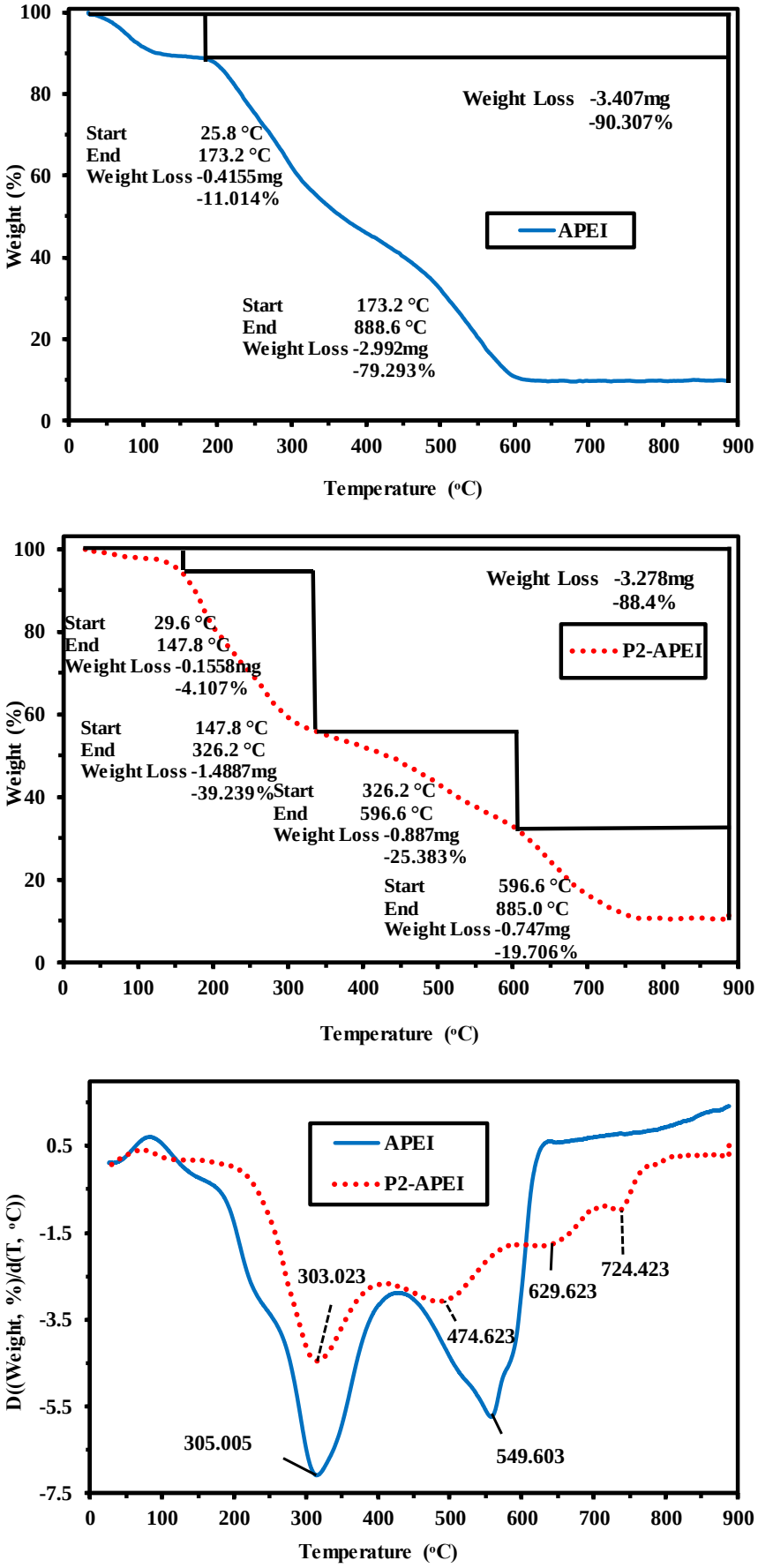

Figure S2. Thermogravimetric analysis of APEI and P2-APEI sorbents.

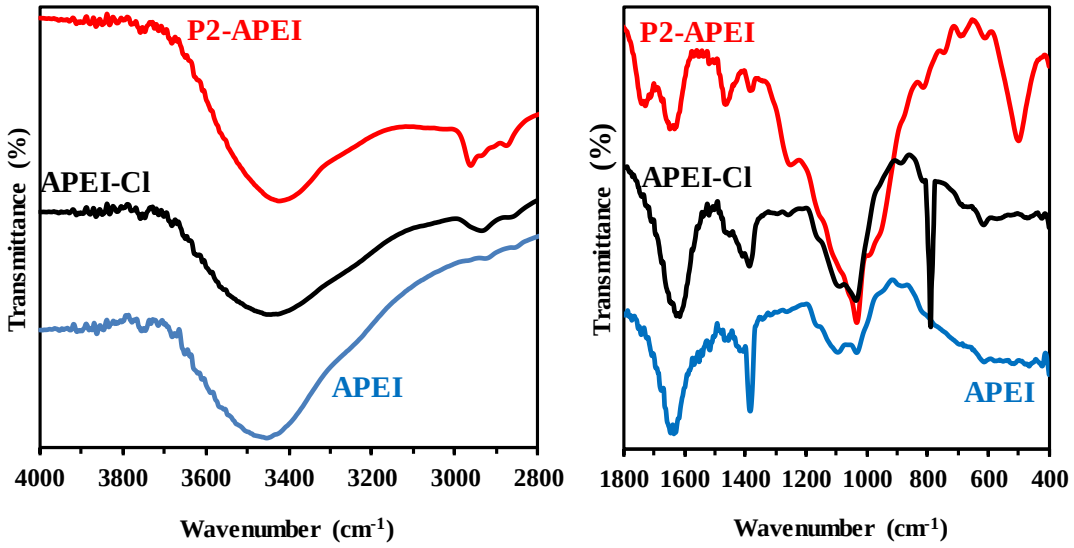

Figure S3. FTIR spectra of APEI, activated APEI (chloromethylated APEI, APEI-Cl) and phosphorylated APEI (P2-APEI) beads (focus on selected wavenumber ranges).

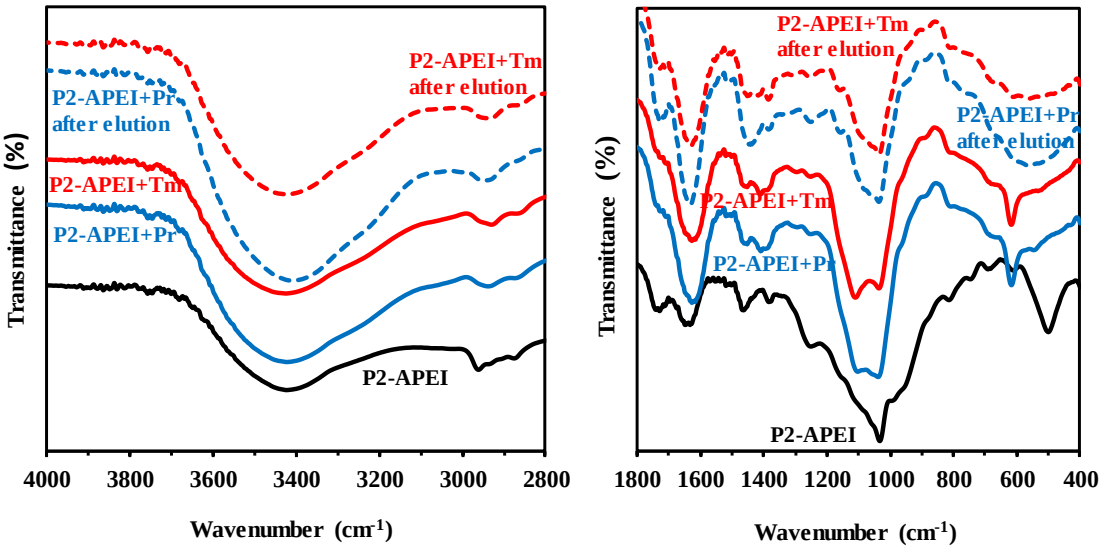

Figure S4. FTIR spectra of sorbents (before and after metal sorption, and after regeneration) (focus on specific wavenumber ranges).

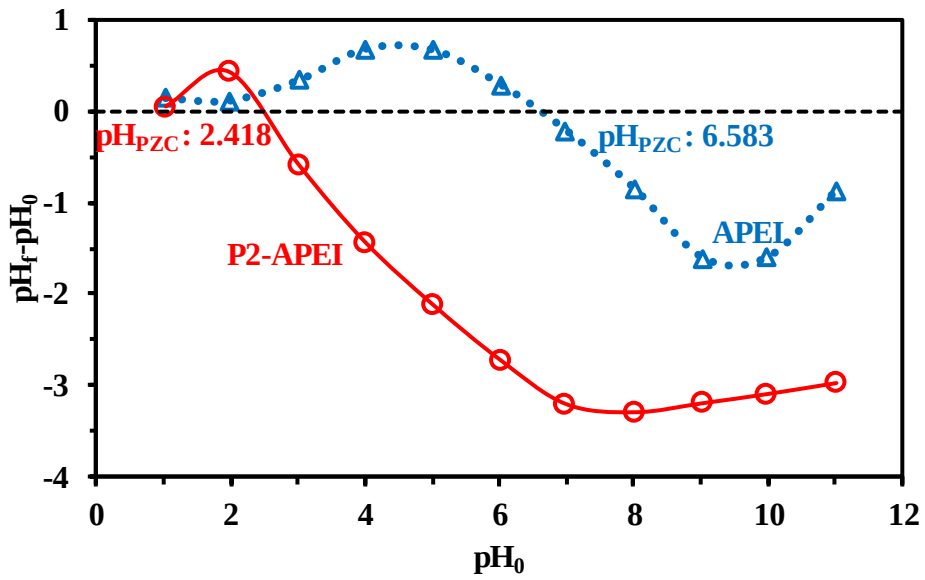

Figure S5. Determination of pH_{PZC} for APEI and P2-APEI sorbents (pH drift method; background salt: 0.1 M NaCl; Sorbent dosage, SD: 2 g L^{-1}; contact time: 48 h).

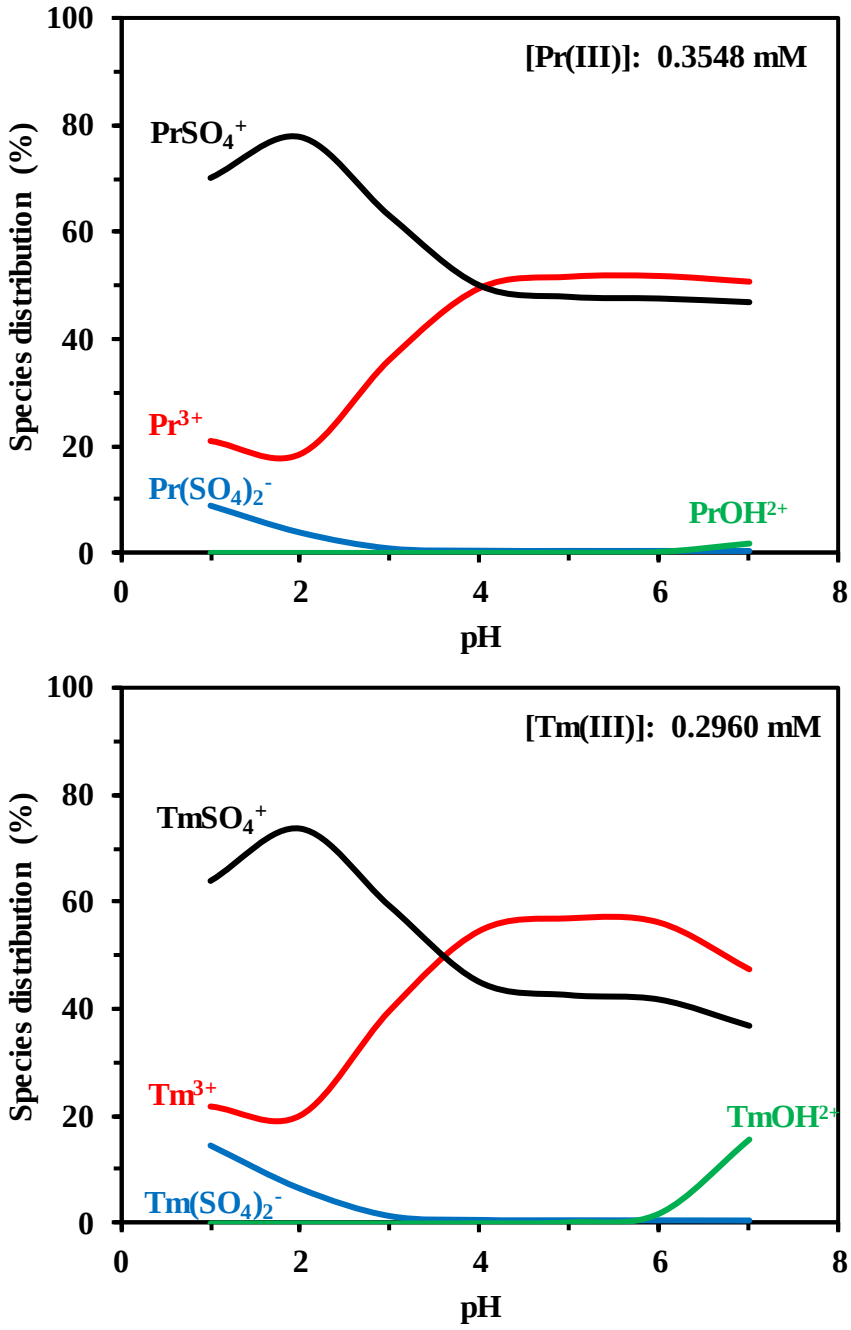

Figure S6. Pr(III) and Tm(III) speciation diagrams (experimental conditions used for the study of pH effect).

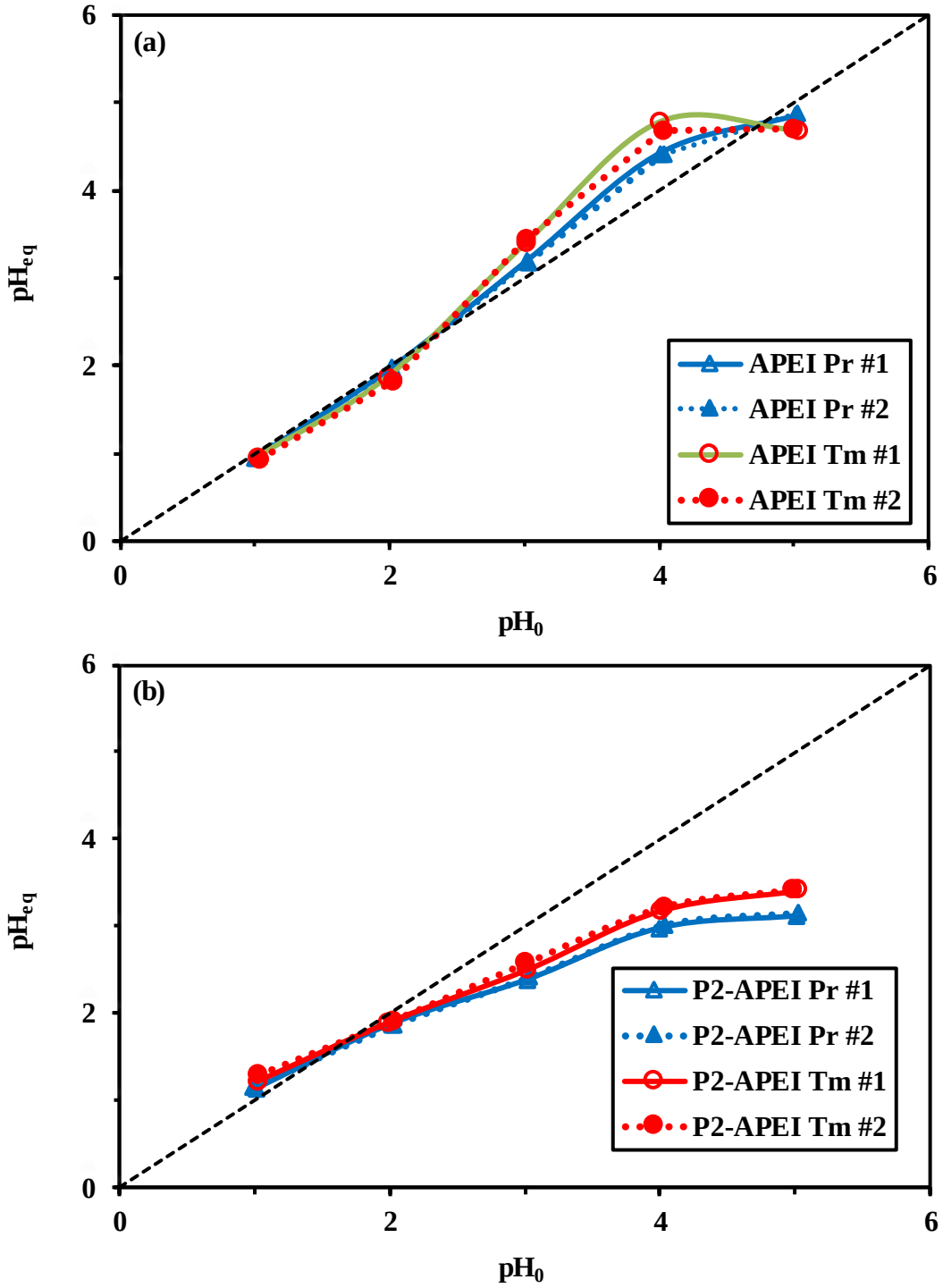

Figure S7. pH variation during Pr(III) and Tm(III) sorption using APEI (a) and P2-APEI (b) sorbents (C_0: 50 mg L^{-1}; Sorbent dosage, SD: 1 g L^{-1}; Contact time: 48 h; T: 22 ±1 °C; duplicate experiments).

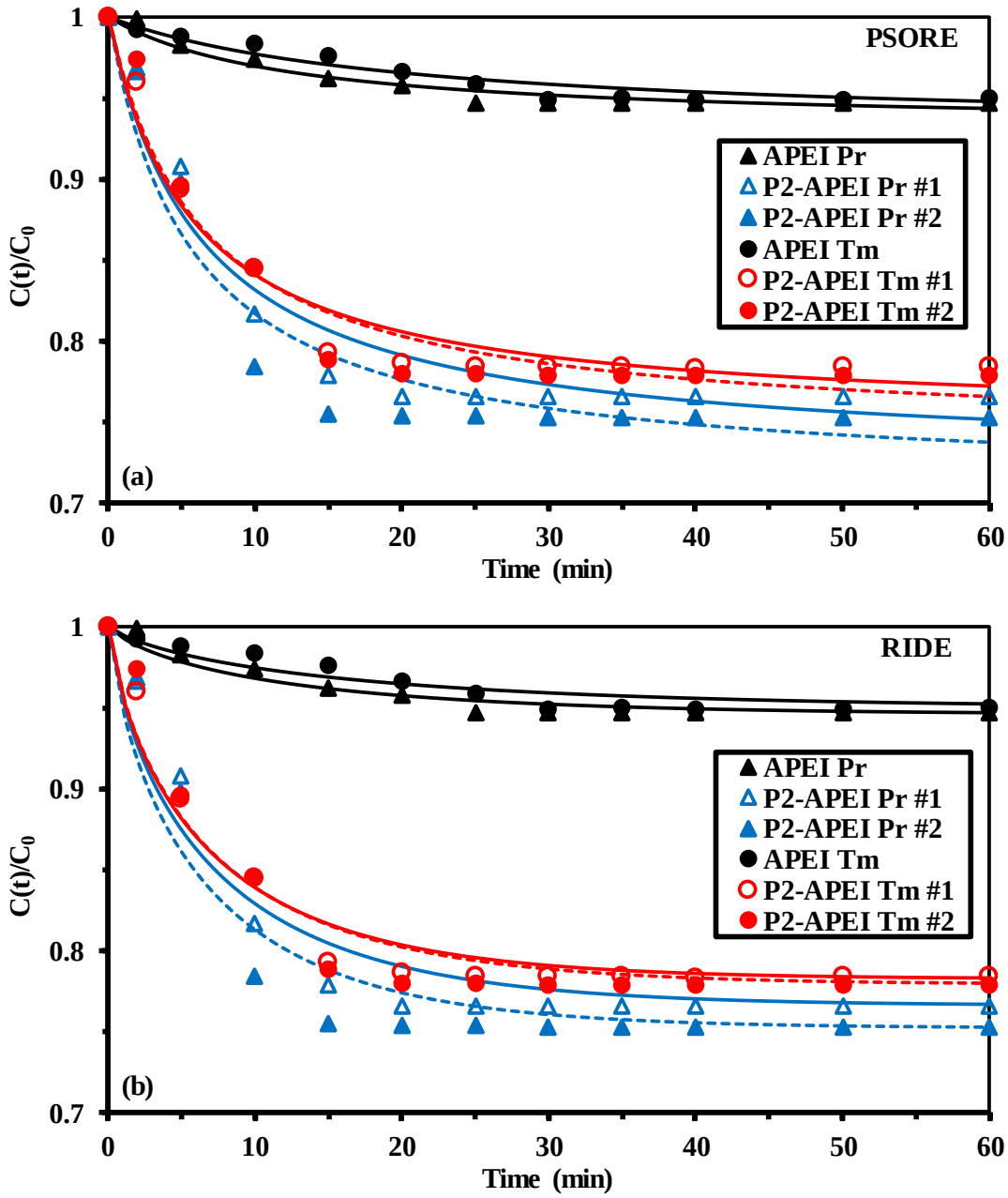

Figure S8a. Pr(III) and Tm(III) uptake kinetics using APEI and P2-APEI sorbents (duplicate experiments) (C_0: 50 mg L^{-1}; Sorbent dosage, SD: 0.25 g L^{-1}; pH_0: 5; pH_{eq}: 4.87 and 4.62 for APEI for Pr(III) and Tm(III), respectively; 3.24-3.12 for Pr(III) and 3.44-3.47 for Tm(III) with P2-APEI; T: 22 ±1 °C; solid lines: modeling with PSORE (a) and RIDE (b)).

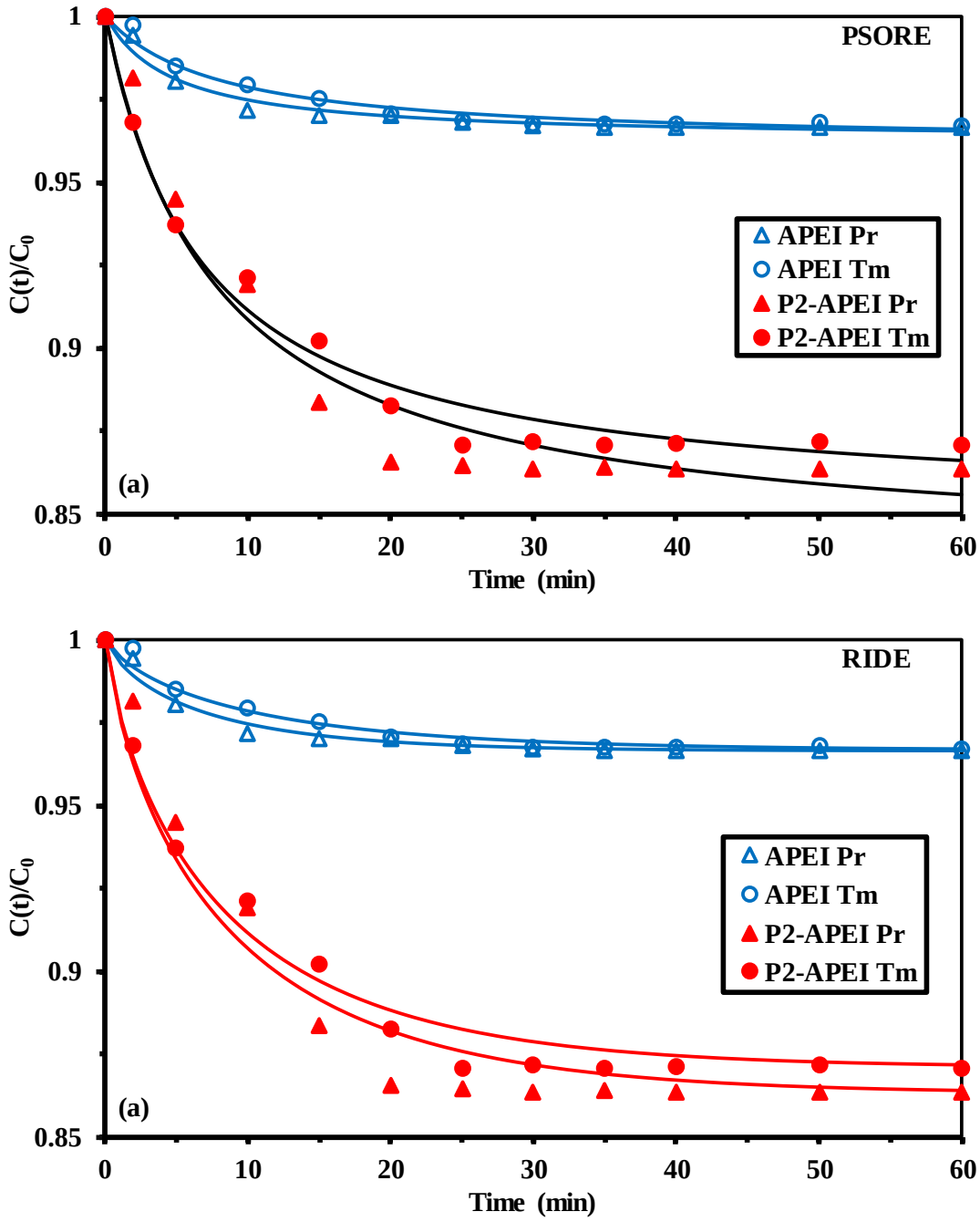

Figure S8b. Pr(III) and Tm(III) uptake kinetics using APEI and P2-APEI sorbents from binary solutions (C_0: 50 mg L^{-1}; Sorbent dosage, SD: 0.25 g L^{-1}; pH_0: 5; pH_{eq}: 4.87 and 4.62 for APEI for Pr(III) and Tm(III), respectively; 3.24-3.12 for Pr(III) and 3.44-3.47 for Tm(III) with P2-APEI; T: 22 ±1 °C; solid lines: modeling with PSORE(a) and RIDE (b)).

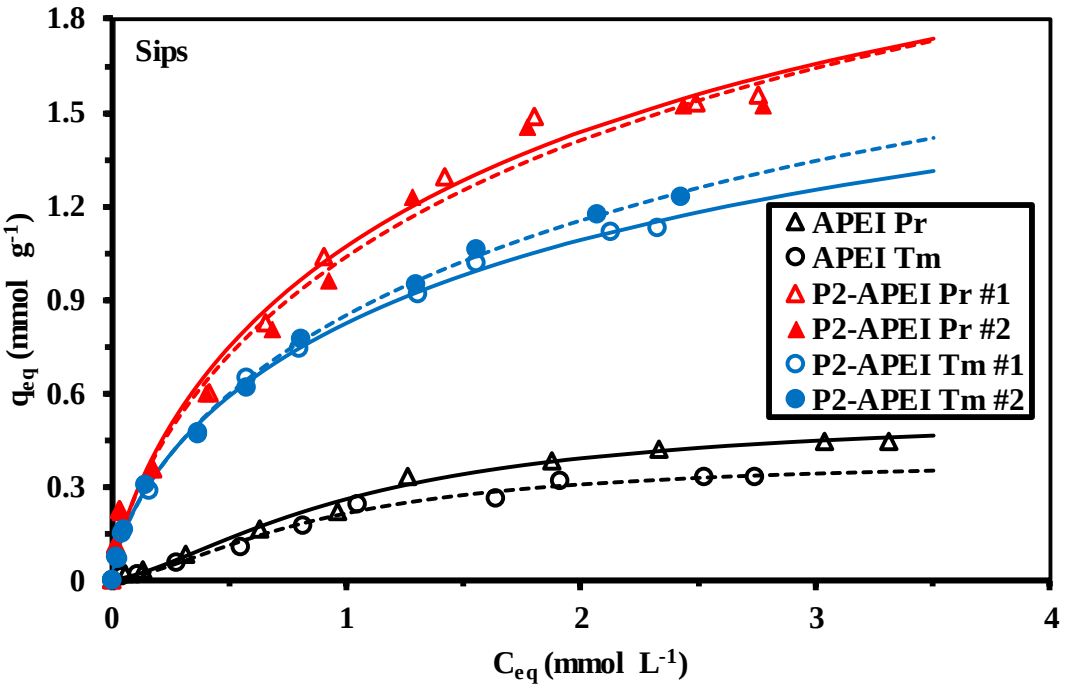

Figure S9. Pr(III) and Tm(III) sorption isotherms using APEI and P2(APEI (duplicate experiments) (C_0: 10-500 mg L^{-1}; Sorbent dosage, SD: 0.5 g L^{-1}; pH_0: 5; pH_{eq}: 4.81-4.7 and 4.79-4.72 for APEI for Pr(III) and Tm(III), respectively; 3.27-3.08 for Pr(III) and 3.54-3.39 for Tm(III) with P2-APEI; time: 48 h; T: 22 ±1 °C; solid lines: modeling with the Sips equation).

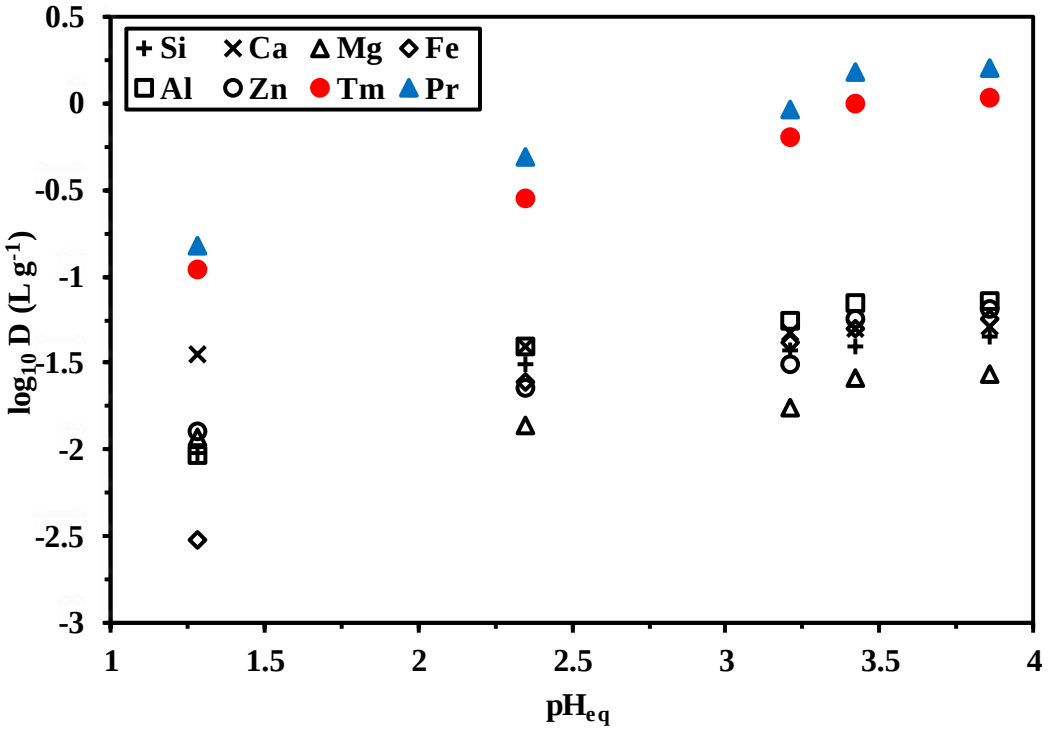

Figure S10. Effect of pH_{eq} on the distribution ratio of selected metals (log_{10} D plots) **(**equimolar 1 mM solutions; SD: 0.5 g L^{-1}; contact time: 48 h; T: 22 ±1 °C).

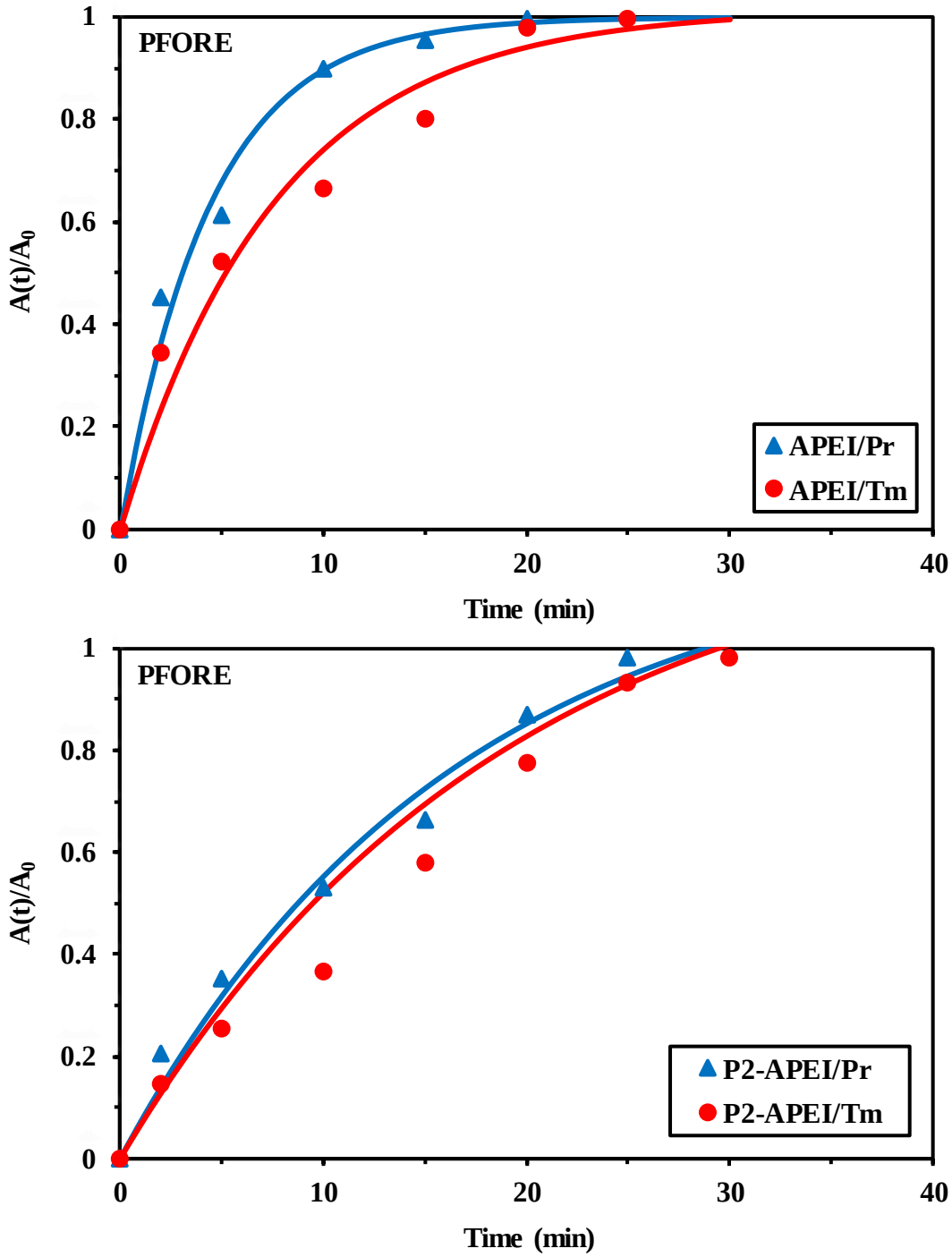

Figure S11. Pr(III) and Tm(III) desorption kinetics for APEI and P2-APEI from binary solution – Modeling with the PFORE (loaded sorbents collected from uptake kinetics; desorption using 0.2 M HCl/0.5 M $CaCl_2$; SD: 1 g L^{-1}, T: 22 ±1 °C; $A(t)/A_0$: metal amount desorbed referred to initial sorbed amount).

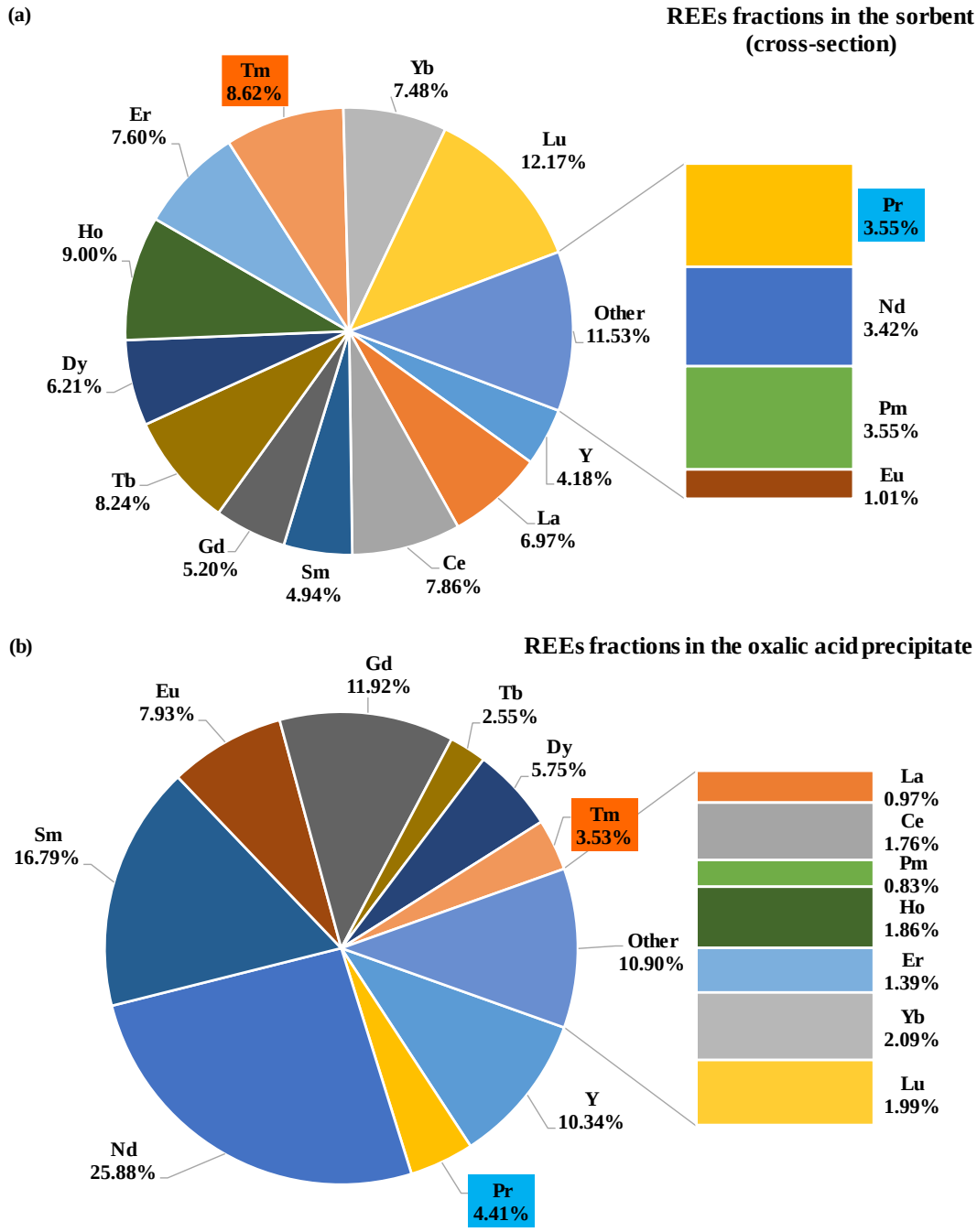

Figure S12. Relative percentages of the different REEs in the sorbent (cross-section) at pH_0: 5, (a)) and in the oxalic acid precipitate (b) (semi-quantitative EDX analysis).

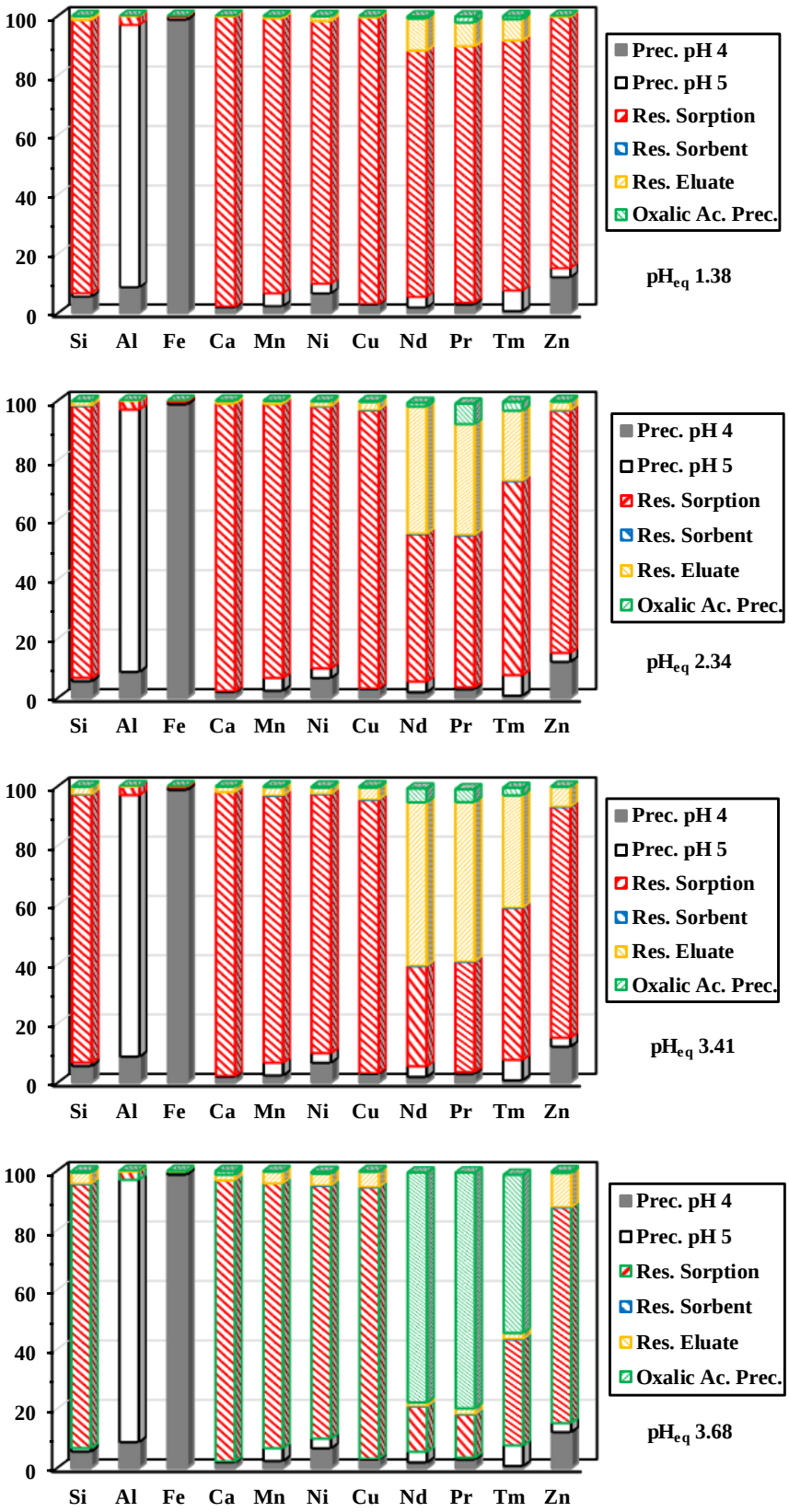

Figure S13. Distribution of selected metals in the different compartments of the global treatment process (pH 4 precipitate (Fe); pH 5 precipitate (Al); residual solution after sorption at different pH_0 values (Res. Sorption); metal residue on the sorbent after elution (Res. Sorbent), Residue in the eluate and the oxalic acid precipitate).

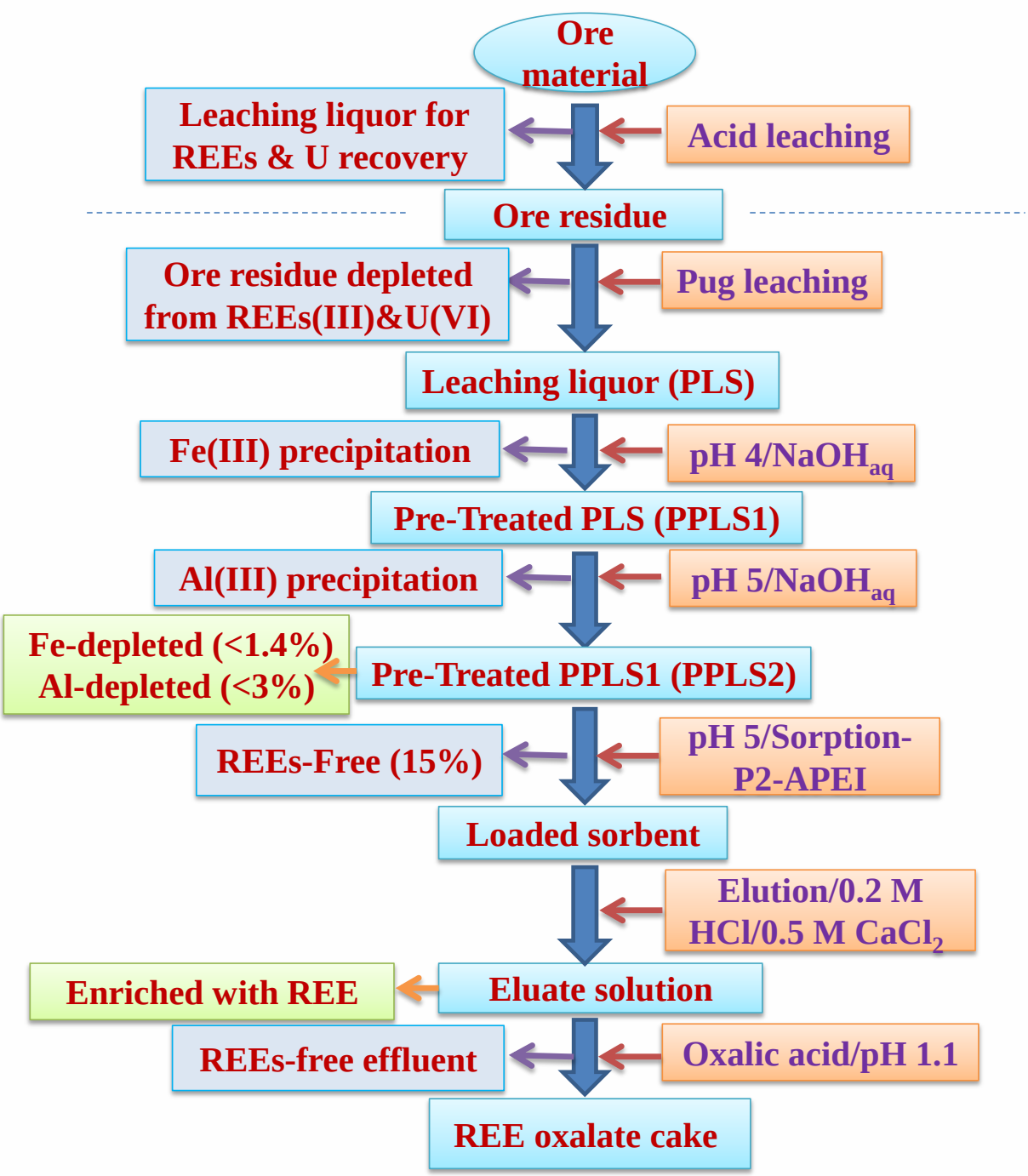

Scheme S1. Proposed flow sheet for the treatment of ore residue.

References

[1] Y.S. Ho, G. McKay, Pseudo-second order model for sorption processes, Process Biochem., 34 (1999) 451-465.
[2] C. Tien, Adsorption Calculations and Modeling, Butterworth-Heinemann, Newton, MA, 1994
[3] R. Zhang, T. Leiviska, Surface modification of pine bark with quaternary ammonium groups and its use for vanadium removal, Chem. Eng. J., 385 (2020) Art. N° 123967.
[4] H.M.F. Freundlich, Uber die adsorption in lasungen, Z. Phys. Chem., 57 (1906) 385-470.

[5] M.I. Temkin, V. Pyzhev, Kinetics of ammonia synthesis on promoted iron catalysts, Acta Physiochim., 12 (1940) 217-222.
[6] O. Falyouna, O. Eljamal, I. Maamoun, A. Tahara, Y. Sugihara, Magnetic zeolite synthesis for efficient removal of cesium in a lab-scale continuous treatment system, J. Colloid Interface Sci., 571 (2020) 66-79.
[7] M.F. Hamza, M.M. Aly, A.A.H. Abdel-Rahman, S. Ramadan, H. Raslan, S. Wang, T. Vincent, E. Guibal, Functionalization of magnetic chitosan particles for the sorption of U(VI), Cu(II) and Zn(II)—Hydrazide derivative of glycine-grafted chitosan, Materials, 10 (2017) 539-560.
[8] J. Coates, Interpretation of Infrared Spectra, A Practical Approach, Encyclopedia of Analytical Chemistry, John Wiley & Sons, Ltd.2006, pp. 1-23.
[9] J. Coates, Interpretation of Infrared Spectra, A Practical Approach, in: R.A. Meyers (Ed.) Encyclopedia of Analytical Chemistry, John Wiley & Sons Ltd, Chichester, U.K., 2000, pp. 10815-10837.
[10] N. Mohammadi, A. Ganesan, C.T. Chantler, F. Wang, Differentiation of ferrocene D-5d and D-5h conformers using IR spectroscopy, J. Organomet. Chem., 713 (2012) 51-59.
[11] N.B. Colthup, L.H. Daly, S.E. Wiberley, Introduction to Infrared and Raman Spectroscopy, 3rd. ed. ed., Academic Press, Inc., San Diego, CA (USA), 1990.
[12] X.J. Hu, J.S. Wang, Y.G. Liu, X. Li, G.M. Zeng, Z.L. Bao, X.X. Zeng, A.W. Chen, F. Long, Adsorption of chromium (VI) by ethylenediamine-modified cross-linked magnetic chitosan resin: Isotherms, kinetics and thermodynamics, J. Hazard. Mater., 185 (2011) 306-314.
[13] Y. Chen, J. Geng, Y. Zhuang, J. Zhao, L. Chu, X. Luo, Y. Zhao, Y. Guo, Preparation of the chitosan grafted poly (quaternary ammonium)/Fe_3O_4 nanoparticles and its adsorption performance for food yellow 3, Carbohydr. Polym., 152 (2016) 327-336.
[14] A.B.D. Nandiyanto, R. Oktiani, R. Ragadhita, How to read and interpret FTIR spectroscope of organic material, Indones. J. Sci. Technol., 4 (2019) 97-118.
[15] A.P. Dean, M.C. Martin, D.C. Sigee, Resolution of codominant phytoplankton species in a eutrophic lake using synchrotron-based Fourier transform infrared spectroscopy, Phycologia, 46 (2007) 151-159.
[16] M. Giordano, M. Kansiz, P. Heraud, J. Beardall, B. Wood, D. McNaughton, Fourier transform infrared spectroscopy as a novel tool to investigate changes in intracellular macromolecular pools in the marine microalga *Chaetoceros muellerii* (Bacillariophyceae), J. Phycol., 37 (2001) 271-279.
[17] L.G. Benning, V.R. Phoenix, N. Yee, M.J. Tobin, Molecular characterization of cyanobacterial silicification using synchrotron infrared micro-spectroscopy, Geochim. Cosmochim. Acta, 68 (2004) 729-741.
[18] M. Cochez, M. Ferriol, J.V. Weber, P. Chaudron, N. Oget, J.L. Mieloszynski, Thermal degradation of methyl. methacrylate polymers functionalized by phosphorus-containing molecules - I. TGA/FT-IR experiments on polymers with the monomeric formula $CH_2C(CH_3)C(O)OCHRP(O)(OC_2H_5)_2$ (R=H, $(CH_2)_4CH_3$, C_6H_5Br, $C_{10}H_7$), Polym. Degrad. Stab., 70 (2000) 455-462.
[19] Z. Zhao, X. Xie, Z. Wang, Y. Tao, X. Niu, X. Huang, L. Liu, Z. Li, Immobilization of *Lactobacillus rhamnosus* in mesoporous silica-based material: An efficiency continuous cell-recycle fermentation system for lactic acid production, J. Biosci. Bioeng, 121 (2016) 645-651.
[20] M. Namdeo, S.K. Bajpai, Chitosan-magnetite nanocomposites (CMNs) as magnetic carrier particles for removal of Fe(III) from aqueous solutions, Colloids Surf., A, 320 (2008) 161-168.

[21] K. Oshita, T. Takayanagi, M. Oshima, S. Motomizu, Adsorption behavior of cationic and anionic species on chitosan resins possessing amino acid moieties, Anal. Sci., 23 (2007) 1431-1434.
[22] X. Zhang, C. Jiao, J. Wang, Q. Liu, R. Li, P. Yang, M. Zhang, Removal of uranium(VI) from aqueous solutions by magnetic Schiff base: Kinetic and thermodynamic investigation, Chem. Eng. J., 198 (2012) 412-419.
[23] M.F. Hamza, J.-C. Roux, E. Guibal, Uranium and europium sorption on amidoxime-functionalized magnetic chitosan micro-particles, Chem. Eng. J., 344 (2018) 124-137.